



## Review Article

# Intra-continental earthquake swarms in West-Bohemia and Vogtland: A review

T. Fischer<sup>a,b,\*</sup>, J. Horálek<sup>a</sup>, P. Hrubcová<sup>a</sup>, V. Vavryčuk<sup>a</sup>, K. Bräuer<sup>c</sup>, H. Kämpf<sup>d</sup>

<sup>a</sup> Institute of Geophysics, Academy of Sciences, Prague, Czech Republic

<sup>b</sup> Charles University in Prague, Faculty of Science, Czech Republic

<sup>c</sup> UFZ Helmholtz Centre for Environmental Research, Halle, Germany

<sup>d</sup> German Research Centre for Geoscience (GFZ), Potsdam, Germany

## ARTICLE INFO

## Article history:

Received 15 March 2013

Received in revised form 24 October 2013

Accepted 3 November 2013

Available online 12 November 2013

## Keywords:

Earthquake swarm

Fluid

West Bohemia

Vogtland

Earthquake triggering

## ABSTRACT

Earthquake swarms and high CO<sub>2</sub> flow of mantle origin are the characteristic features of West Bohemia/Vogtland (Central Europe). At present, the highest concentration of earthquake activity and CO<sub>2</sub> degassing occurs in the area of the Cheb Basin at the intersection of the Eger Rift and Regensburg–Leipzig–Rostock Zone with three Quaternary active volcanoes. We review about 140 studies on structure, tectonics, volcanism, seismicity, earthquake source, triggering mechanisms, and gas-isotope geochemistry focused on the earthquake swarms from this area with the aim to build a complex image of the ongoing processes and find a possible link between activity of the mantle-derived fluids and the earthquake swarms. The so far unpublished data on the 2011 swarm and little known data on the 1824 swarm are presented, as well, showing that earthquake swarms activate a complex fault system and display long-term migration that differs from the occurrence of CO<sub>2</sub> escapes. The activity of individual swarms is consistent with models involving high-pressure fluids; the isotopic signature of the rising gas proves its origin at depths below the hypocenters. We show that the earthquake swarms and degassing of CO<sub>2</sub> of magmatic origin represent common result of the geodynamic activity of the area. Nevertheless, current knowledge does not preclude processes other than fluid-induced failure in triggering swarm seismicity.

© 2013 Elsevier B.V. All rights reserved.

## Contents

1. Introduction	2
2. Tectonic setting	2
2.1. Neotectonic activity	2
2.2. Volcanic activity	5
2.3. Summary	5
3. Structure studies	5
3.1. Active seismic experiments	5
3.2. Passive seismic investigations	5
3.3. Anisotropy of the crust	6
3.4. Upper mantle dynamics – seismic tomography and xenolith studies	6
3.5. Summary	8
4. Earthquake swarms	8
4.1. Swarm observations in the past	8
4.2. Instrumentally recorded swarm activity	9
4.3. Earthquake swarms in the Nový Kostel focal zone	9
4.4. Earthquake source studies	10
4.5. Summary	12
5. Earthquake source mechanisms and stress field	13
5.1. Focal mechanisms and their occurrence during swarms	13

\* Corresponding author.

E-mail address: [fischer@natur.cuni.cz](mailto:fischer@natur.cuni.cz) (T. Fischer).

5.2.	Detailed geometry of the Nový Kostel focal zone	13
5.3.	Tectonic stress and principal focal mechanisms	14
5.4.	Non-double-couple components and their origin	15
5.5.	Summary	16
6.	Fluids in the lithosphere and the earthquake swarms	16
6.1.	Regional distribution pattern and origin of CO <sub>2</sub> degassing in West Bohemia/Vogtland	16
6.2.	Possible relation of the fluid signature to seismic and magmatic activity	16
6.3.	Possible relation of groundwater regime and gas flow with seismic activity	17
6.4.	Summary	19
7.	Earthquake swarm triggering	19
7.1.	Correlation of seismicity in the whole West-Bohemia/Vogtland	19
7.2.	Swarm triggering as a result of elastic stress transfer	19
7.3.	Migration of hypocenters and fluid and magma triggering	20
7.4.	Other models of the swarms	21
7.5.	Summary	22
8.	Discussion and conclusions	22
8.1.	Summary of the existing results	22
8.2.	A broader view of the geodynamics in time and space	23
8.3.	Concluding remarks and prospects for further research	24
	Acknowledgments	24
	References	25

## 1. Introduction

The West Bohemia/Vogtland earthquake swarm region is one of the unique European intra-continental areas that display present activity of geodynamic processes, in particular, degassing of CO<sub>2</sub> and persistent seismic activity. The degassing of CO<sub>2</sub> of deep origin occurs in the form of CO<sub>2</sub>-rich mineral waters and in the form of wet and dry mofettes in several degassing fields. The former represents the basis for multiple spa resorts distributed along the neighboring regions of the Czech Republic and Germany. The high <sup>3</sup>He/<sup>4</sup>He ratios point to the mantle origin of the ascending gases. Seismicity is dominated by periodically occurring earthquake swarms with seismic magnitudes not exceeding M<sub>L</sub> 5; a culmination of seismicity is observed within the last 30 years when a single M<sub>L</sub> 4 + swarm and multiple M<sub>L</sub> 3 + swarms occurred. These processes have been intensively studied by many authors and from various viewpoints, which resulted in a common opinion that the seismic activity stems from the whole geodynamic activity in the region; though the triggering factors still remain undisclosed.

In this review we summarize the seismological, structural and gas-emission studies carried out in West Bohemia and Vogtland with the aim to critically evaluate possible relations between seismic swarm activity and deep geodynamic processes. The paper is organized according to the individual disciplines and each section is concluded by a short summary outlining the key results that contribute to build up a comprehensive view of the present geodynamic processes in this unique European natural laboratory.

## 2. Tectonic setting

The Bohemian Massif is one of the largest stable outcrops of pre-Permian rocks in Central and Western Europe. It forms the easternmost part of the Variscan orogenic belt, which developed approximately between 500 and 250 Ma during a period of large-scale crustal convergence, collision of continental plates and microplates and subduction (Matte et al., 1990). The West Bohemia/Vogtland region (Fig. 1) forms the western part of the Bohemian Massif and it is situated in the transition zone among three different Variscan structural units: the Saxothuringian in the north-west, the Teplá-Barrandian in the central region, and the Moldanubian in the south-east (Babuška et al., 2007). The Paleozoic suture between the Saxothuringian and the Teplá-Barrandian with the Moldanubian units has been reactivated since the lower Triassic. The post-orogenic extension, together with the alkaline magmatic activity during the Cenozoic led, to the evolution of the Eger Rift, a 300 km long and 50 km wide ENE–WSW trending zone as an active element of the European Cenozoic Rift System

(Prodehl et al., 1995). This tectonosedimentary structure is associated with a system of Cenozoic sedimentary basins and intense intraplate alkaline volcanism (Ulrych et al., 2011).

### 2.1. Neotectonic activity

The area is located at the intersection of two tectonic structures: the ENE–WSW striking Eger Rift (EGR) with the Eger Graben (EG) in the center and the N–S striking Regensburg–Leipzig–Rostock Zone, (length: 700 km and width: 40 km) which is seismically active in its middle part between Mariánské Lázně/Marktredwitz and Leipzig (Bankwitz et al., 2003), Fig. 2. This zone is dominated by numerous N–S faults, which are composed of en echelon segments measuring a few kilometers. The middle part consists of a set of sub-parallel faults, which were partly detected from satellite images and from negative geomorphological forms (Krentz et al., 1996; Krull and Schmidt, 1990). The faults were observed in numerous uranium mining exposures (including boreholes and prospecting trenches), especially in W Saxony and E Thuringia, Germany (Bankwitz et al., 2003).

The Cheb–Domažlice Graben (CDG) is located in the eastern part of the Regensburg–Leipzig–Rostock Zone (Fig. 2) and to the east it is bounded by the approximately 100 km long Mariánské Lázně Fault (MLF), which is morphologically expressed by a 50–400 m high escarpment. The western flank of the graben is characterized by a more gentle topography. The formation of the Cheb Basin in the northern part of CDG was initiated by the reactivation of basement faults inherited from the Variscan orogeny during the late Oligocene–Miocene. The sedimentary fill of the Cheb Basin consists of Tertiary and Quaternary sediments up to 300 m thick, representing debris of Proterozoic and Paleozoic magmatic and metamorphic rocks of the north-western Bohemian Massif, that bound the basin (Fiala and Vejnar, 2004). Sedimentation started during the Late Eocene, was interrupted in the Lower Oligocene and continued from Late Oligocene to Miocene; after a period of erosion it was revived in the Pliocene. The normal character of the fault zone controlled the formation of the Cheb Basin since late Eocene until Pliocene (Špičáková et al., 2000). The Cheb Basin is typified by a blocky fabric with a network of faults of different orientation (trending in NNW, NW, NW, E–W and N–S directions). Among them, the NNW trending faults are dominant; these faults belong to the East Marginal Fault of the basin that forms the northern portion of the MLF. The N–S trending faults do not seem to have significantly influenced the basin fill geometry (Špičáková et al., 2000 and references therein).

The NNW–SSE striking Mariánské Lázně Fault (MLF) intersects the area close to the main seismically active zone of Nový Kostel (NK), where more than 80% of seismic energy was released within the last

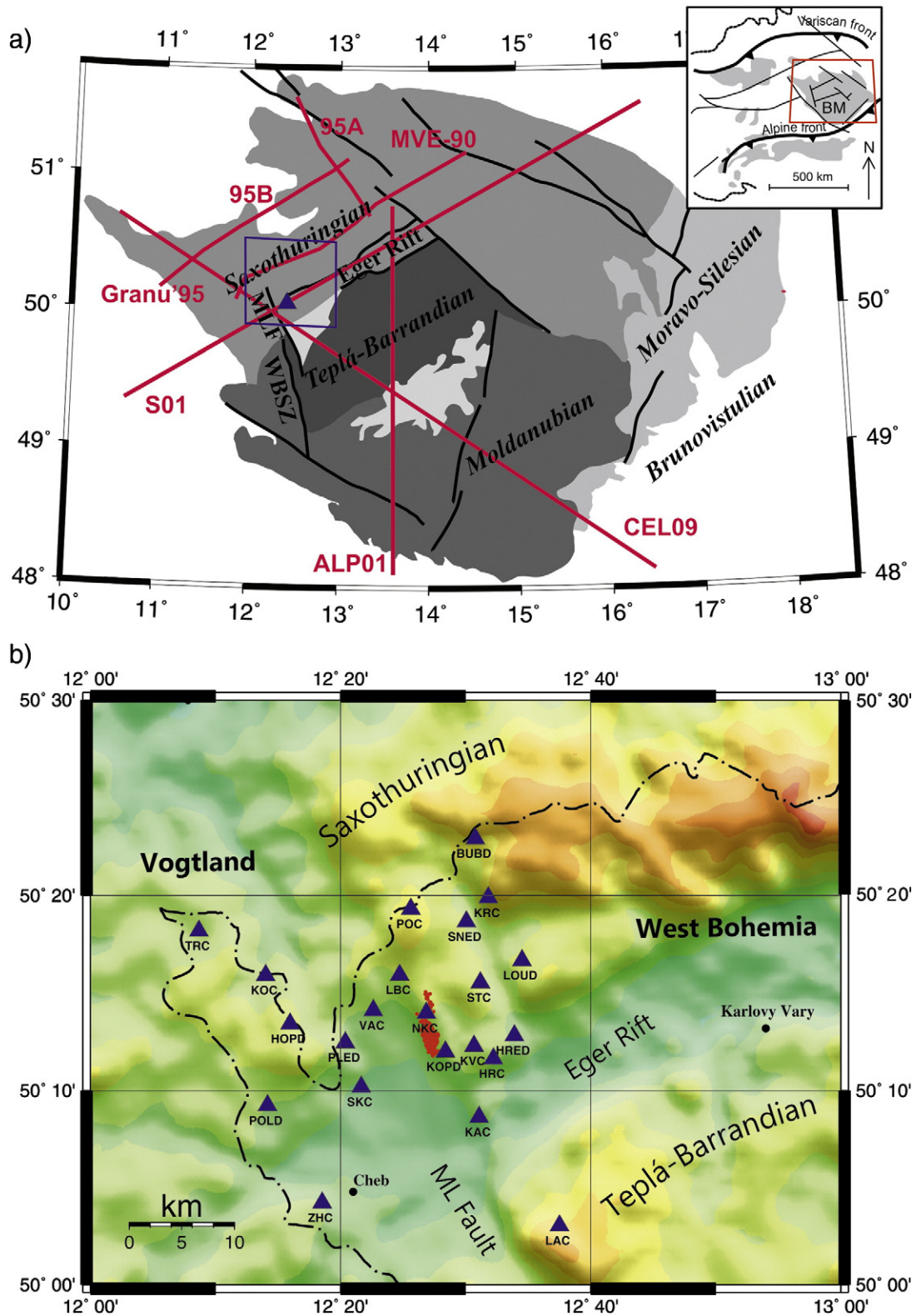


**Fig. 1.** (a) Simplified sketch of tectonic units of the Bohemian Massif (BM) (modified after Babuška and Plomerová, 2013) with major seismic profiles (red lines) in the West Bohemia/Vogtland area. (b) Topographic map of the West Bohemia/Vogtland region. Seismic stations of the WEBNET network are marked by blue triangles; hypocenters of local micro-earthquakes of the 2008 swarm marked by red dots. ML Fault - Mariánské Lázně Fault.

25 years (Fischer and Michálek, 2008). Another active fault system trends N–S (Bankwitz et al., 2003) and is aligned with the hypocenters in the Nový Kostel area with a strike of about 170° (Fischer et al., 2010). Bankwitz et al. (2003) discuss this system in the context of seismicity in central and western Europe and delimit the N–S trending

Počátky–Plesná zone (PPZ) to be a part of the main earthquake line, the Regensburg–Leipzig–Rostock Zone (Fig. 2). According to geological observations of Škvor and Satran (1974), Bankwitz et al. (2003) assumed that the Nový Kostel seismicity has been active since 10 ka as minimum age or since 120 ka as maximum age. According to Peterek

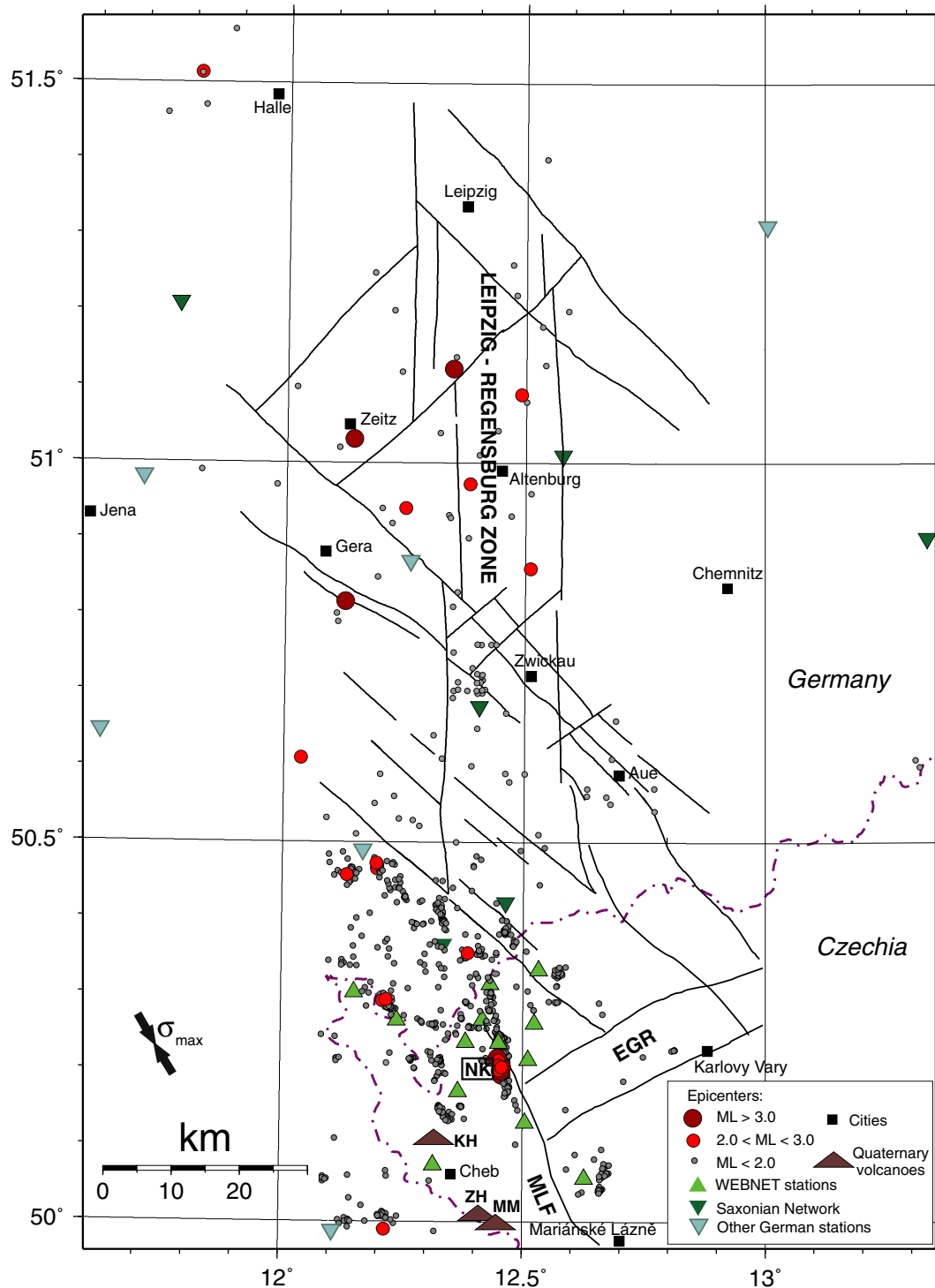


**Fig. 2.** The West Bohemia/Vogtland earthquake swarm region as a part of the Leipzig–Regensburg seismoactive zone with the earthquake epicenters for the 1991–2011 period (gray and red circles) and major faults (full lines). The main focal zone Nový Kostel (NK) is situated at an intersection of the Eger Rift (EGR) and Mariánské Lázně fault (MLF). Nearby volcanoes Komorní Hůrka (KH) and Železná Hůrka (ZH) are denoted by blue stars, Mýtina Maar is located close to ZH. The maximum compression in the region striking 145° is indicated in the lower left corner. Triangles indicate seismic stations of the (WEBNET – green, apex up, SXNET – dark green, apex down, other stations – green-blue, apex down). Black squares denote towns. The Czech–German border is marked by dashed line.

et al. (2011), the neotectonic activity of the southern section of the PPZ at Nebanice started about 475 ka (maximum age) or 145 ka (minimum age). They interpreted PPZ as a part of sinistral wrench zone that branches the MLF in four individual segments between Mariánské Lázně and Luby.

Two geophysical studies were recently targeted to reveal the fault fabric of the Cheb Basin in detail. Flechsig et al. (2010) applied electrical resistivity tomography (ERT) method at two sites on the active

fault zones in the Nový Kostel area, the PPZ and the MLF. The models of resistivity distributions down to a depth of 50–80 m reveal a graben-like structure of the MLF with vertical displacements of ~10–15 m. The resistivity sections of similar depth range crossing the PPZ show mainly NE dipping vertical features of higher conductivity, which suggests high permeability of these structures. Fischer et al. (2012) applied the ERT method and 3D version of ground penetrating radar (GPR) to extend the geological information gathered



from a trench survey that exposed the MLF in the Nový Kostel area. A family of five faults striking NW and NNW was found to intersect a high-resistivity sand–gravel body. A right-lateral displacement was identified along one of the NW striking faults based on a detailed analysis of 3-D GPR cube. A paleo-seismologic survey is carried out in order to learn about possible seismic activity of the MLF during the Holocene.

The surface movement due to the present tectonic processes was subject to several studies. According to [Wendt and Dietrich \(2003\)](#) the results of five GPS campaigns carried out from 1994 to 2001 in the German part of the West Bohemia/Vogtland region revealed significant relative horizontal displacements of up to 5 mm between observation epochs. GPS campaigns and continuous observations in the Czech sites during 1993–2007 ([Mrlina and Seidl, 2008](#)) indicated horizontal displacements of few mm and no clear long-term trend; annual precise leveling campaigns revealed regular vertical displacements only during some of the earthquake swarms. [Schenk et al. \(2009\)](#) showed that differential velocities obtained from the continuous monitoring at five permanent GPS stations in West Bohemia during 2003–2005 did not exceed 1 mm/year in horizontal and 2 mm/year in vertical directions at stations more than 10 km apart. However, the resulting surface movements presented in these two studies are at the bound of the error of the geodetic methods and thus they do not allow for more detailed analyses. The near-field static displacement due to the strongest events of the 2008 swarms was only of the order of  $10^{-5}$  m as found by [Zahradník and Plešinger \(2010\)](#) in broadband records at seismic station NKC.

## 2.2. Volcanic activity

Volcanic activity was associated with two Quaternary scoria cones: Komorní hůrka/Kammerbühl (KH) and Železná hůrka/Eisenbühl (ZH), and the Mýtina maar (MM) ([Geissler et al., 2004](#); [Mrlina et al., 2007, 2009](#); [Proft, 1894](#); [Seifert and Kämpf, 1994](#)), see Fig. 2. These small volcanoes are located at the flanks of the Eger Rift (Fig. 2) and are situated at the NW–SE striking Tachov fault as the western boundary of the Cheb–Domažlice Graben ([Geissler et al., 2004](#)). The original depth of the recently discovered Mýtina maar is  $\geq 140$  m. The total volume of erupted material and the spatial distribution of the volcanoclastics of the MM are currently unknown.

Two main stages of volcanic activity are recognized at the Quaternary volcanic centers: phreatomagmatic initial stage and eruptive final stage. The lava of the KH, ZH and MM is characterized as olivine-nephelinitic ([Mrlina et al., 2009](#); [Seifert and Kämpf, 1994](#)). Age determinations using different methods indicate that the Quaternary volcanic activities close to the Cheb Basin occurred in the mid-Pleistocene 0.78–0.12 Ma ago ([Mrlina et al., 2007](#); [Šibrava and Havlíček, 1980](#); [Ulrych et al., 2003](#); [Wagner et al., 2002](#)). Another support for the existence of magmatic reservoirs beneath West Bohemia was given by [Vylita et al. \(2007\)](#) who applied the  $^{230}\text{Th}/^{234}\text{U}$  method to the travertine samples from Karlovy Vary. They gave evidence that magmatic  $\text{CO}_2$  escape dates back to about 0.23 Ma.

## 2.3. Summary

The area is intersected by two tectonic structures, the Eger Rift and the Regensburg–Leipzig–Rostock Zone with Tertiary Cheb Basin in the center. A system of faults of various orientations is found in the area and dominated by the Mariánské Lázně Fault. However, no link between the fault in depth delineated by hypocenters in the Nový Kostel zone and faults documented at the surface was found; only the PPZ shows a similar strike as the earthquake cluster. The Quaternary volcanism in West Bohemia/Vogtland is documented in three small volcanoes and is dated 0.78–0.12 Ma ago; an age of  $<0.23$  Ma was found for the onset of  $\text{CO}_2$ -rich hydrothermal activity in one area.

## 3. Structure studies

The concentration of various presently ongoing geodynamic phenomena in a small area of West Bohemia/Vogtland suggests deeper-seated processes and thus indicates the importance of knowledge of crustal and upper mantle structure.

### 3.1. Active seismic experiments

Several seismic experiments have been carried out in this area over the last 25 years. Active seismic studies comprised of reflection experiments such as DEKORP-4/KTB, MVE-90, and 9HR ([Behr et al., 1994](#); [DEKORP Research Group, 1988](#); [Tomek et al., 1997](#)) and the refraction and wide-angle reflection experiments such as GRANU'95 ([Enderle et al., 1998](#)), CELEBRATION 2000 with CEL09 profile ([Hrubcová et al., 2005](#)), ALP 2002 with ALP01 profile ([Brückel et al., 2007](#)), and SUDETES 2003 with S01 profile ([Grad et al., 2008](#)).

In the upper crustal structure, modeling of the refraction profile CEL09 of the CELEBRATION 2000 experiment ([Hrubcová et al., 2005](#)) delimited the area of the amphibolite Mariánské Lázně Complex at the boundary between the Saxothuringian and Barrandian with increased velocities and density contrast. Lower velocities in its close vicinity coincided well with the location of the Karlovy Vary granite massif, which was also confirmed by gravity modeling to a depth of 10 km ([Blecha et al., 2009](#)). Combined data from active experiments and passive local swarm sources led to a 3-D tomography model ([Růžek and Horálek, 2013](#)), which is supposed to be used for updated locations of local earthquakes.

At the lower crustal level, modeling of the refraction and wide-angle reflection profile CEL09 revealed a highly reflective top of the lower crust at a depth of 27–28 km ([Hrubcová et al., 2005](#)), see Fig. 3. These results corresponded well with the reflection profile MVE-90, where the Moho was interpreted at 10 s two-way-time at the bottom of 5–6 km thick reflective lower crust ([DEKORP Research Group, 1994](#)). The existence of a high-velocity layer at the base of the crust, with the top at 24 km, was also indicated in the GRANU'95 results ([Enderle et al., 1998](#)). According to [Geissler et al. \(2005\)](#) all these features of the lower crust may be interpreted as low-angle shear zones containing fluids and/or small magmatic intrusions (sills/dikes) or partial melting.

### 3.2. Passive seismic investigations

Passive seismic experiments with permanent and temporary seismic stations were carried out to study major lithospheric discontinuities with the teleseismic receiver function approach ([Geissler et al., 2005](#); [Heuer et al., 2006](#); [Wilde-Piorko et al., 2005](#)). The receiver functions observed converted waves from the base of the crust at about 3.7 s. With constant average crustal velocity  $V_p$  of  $6.3 \text{ km s}^{-1}$  and  $v_p/v_s$  ratio of 1.73, the depth of the Moho was interpreted at 31 km. Underneath the western part of the Eger Rift, a delay time of only 3.0–3.3 s was interpreted as a crustal thinning to about 27 km ([Geissler et al., 2005](#)). Similar results were obtained by [Heuer et al. \(2006\)](#) who used receiver functions in a dense seismic network and restricted the Moho upwelling at the south-western termination of the Eger Rift.

The differences in the Moho depth from active and passive seismic investigations were explained, to some extent, by different resolutions of these methods, by different frequency bands and spatial resolutions and/or by the uncertainty in the  $v_p/v_s$  ratio. [Hrubcová and Geissler \(2009\)](#) applied joint modeling of the seismic refraction data and receiver functions in West Bohemia/Vogtland. This resulted in a model with lower crustal layer (or gradient zone) of 5 km thickness where its top was at a depth of 28 km and high reflectivity obscured weaker Moho reflections at a depth of ~32–33 km.

The laminated structure of the Moho was also confirmed by [Hrubcová et al. \(2013\)](#) who analyzed reflected/converted phases in the waveforms of local microearthquakes from the 2008 swarm

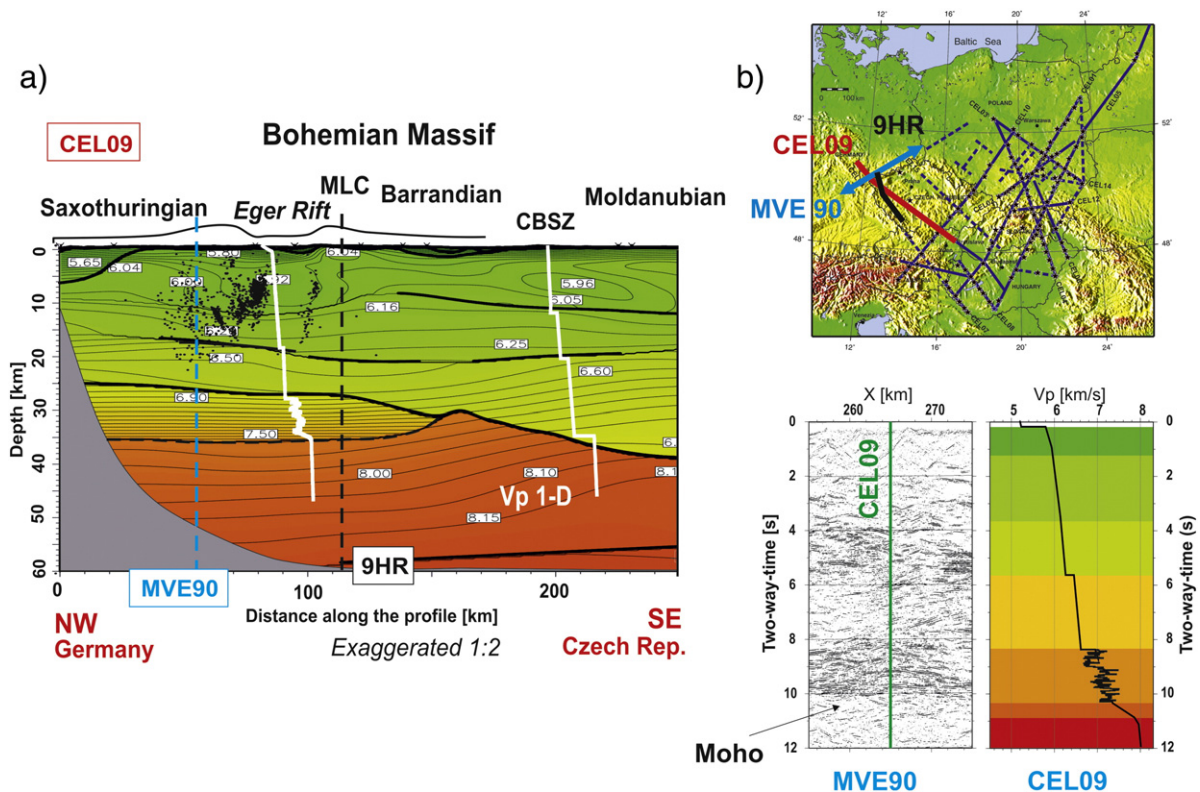


**Fig. 3.** (a) The 2-D model of the P-wave velocity along the CEL09 profile from forward ray-tracing modeling (with SEIS83) (Hrubcová et al., 2005). Bold lines mark boundaries constrained by reflections and well constrained interfaces in the uppermost crust; dashed bold line mark layer boundary where no reflections were observed. Thin lines represent velocity isolines spaced at intervals of  $0.05 \text{ km s}^{-1}$ . Dots show hypocenters of the earthquake swarms in the West Bohemia/Vogtland area. Superimposed are 1-D velocity characteristics for different regions. MLC, Mariánské Lázně Complex; CBSZ, Central Bohemian Shear Zone. Vertical exaggeration is 1:2. (b) Comparison of the reflections along the seismic reflection profile MVE-90 (DEKORP Research Group, 1994) with the 1-D velocity model profile CEL09 (converted to two-way travel time) at the crossing point. Note band of reflectors between 8.2 s and 10 s of two-way travel time at the MVE-90 profile corresponding to the high gradient lower crust in the CEL09 profile.

(Fig. 4). Since the waveforms of microearthquakes are significantly influenced by radiation pattern, the data were processed separately for clusters of earthquakes with similar focal mechanisms. Their new multi-azimuthal approach revealed a reflective zone at the Moho depths with one or two strongly reflective interfaces. The thickness of the zone varied from 2 to 4 km within a depth range of 27–31.5 km and was delimited by reflections from its top and bottom boundaries, sometimes with strong reflectors within the zone (Fig. 4).

### 3.3. Anisotropy of the crust

Shear-wave splitting analysis of waveforms of local microearthquakes revealed that the upper Earth's crust in the West Bohemia/Vogtland region is anisotropic (Vavryčuk, 1993; Vavryčuk and Boušková, 2008). The observed split S waves are usually separated in time and polarized in roughly perpendicular directions in the horizontal projection. In most cases, the polarization of the fast S wave is aligned NW–SE (referred to as “normal splitting”), which is close to the direction of the maximum horizontal compression in the region (see Section 6.3). However, for some stations, the polarization of the fast S wave can also be aligned NE–SW (referred to as “reverse splitting”) or even E–W (see Fig. 5). The pattern of normal/reverse splitting on a focal sphere is station-dependent and indicates the presence of laterally inhomogeneous anisotropy with inclined axes. The presence of inclined anisotropy in the upper crust is confirmed by observations of directionally dependent delay times between the split S waves. The maximum values of the delay time indicate S-wave anisotropy strength of 4–6% provided that anisotropy is distributed along the whole ray path. If not, anisotropy can locally reach values up to 10–15%. A complex and station dependent anisotropy pattern is probably the result of a complicated anisotropic crust composed by diverse geological blocks

characterized by different types of anisotropic rocks such as gneisses, mica schists and phyllites (see Chlupáčová et al., 2003). Note that anisotropic crust is observed also in adjacent areas, for example, in the KTB site (Rabbel, 1994). The rock drilled at the KTB basically consists of alternating felsic and mafic layers, mainly biotite gneiss and amphibolite; the layers are steeply folded with dips between  $60^\circ$  and  $90^\circ$ , with penetrative foliation dipping between  $50^\circ$  and  $80^\circ$  (Rabbel et al., 2004). Dipping anisotropic crustal layers are also indicated using the receiver function analysis of P teleseismic waveforms observed at some German stations (e.g., station MOX) close to the West Bohemia/Vogtland region (see, Eckhardt and Rabbel, 2011).

### 3.4. Upper mantle dynamics – seismic tomography and xenolith studies

As an alternative explanation to the Quaternary rift tectonic model for the area, a ‘plume-like’ low-velocity structure below the Eger Rift was proposed. This was tested by Plomerová et al. (2007) who applied high-resolution teleseismic P-velocity tomography down to a depth of 250 km to characterize the structure of the upper mantle. In contrast to recent findings of small plumes beneath the French Massif Central and the Eifel in Germany (Granet et al., 1995; Ritter et al., 2001), no columnar low-velocity anomaly, which could be interpreted as a mantle plume was found beneath West Bohemia. Alternatively, the anomaly can be interpreted by an upwelling of the lithosphere/asthenosphere boundary reflecting a zone of a lithosphere weakness and stretching at the margins of paleoplates (Babuška et al., 2007; Babuška and Plomerová, 2013). However, using teleseismic receiver functions, Heuer et al. (2011) found that the thickness of the mantle transition zone beneath the western Bohemian Massif is normal, with a faint hint to thinning in the northern part. Their conclusion is that a plume-like structure may exist in the upper mantle below the western Bohemia



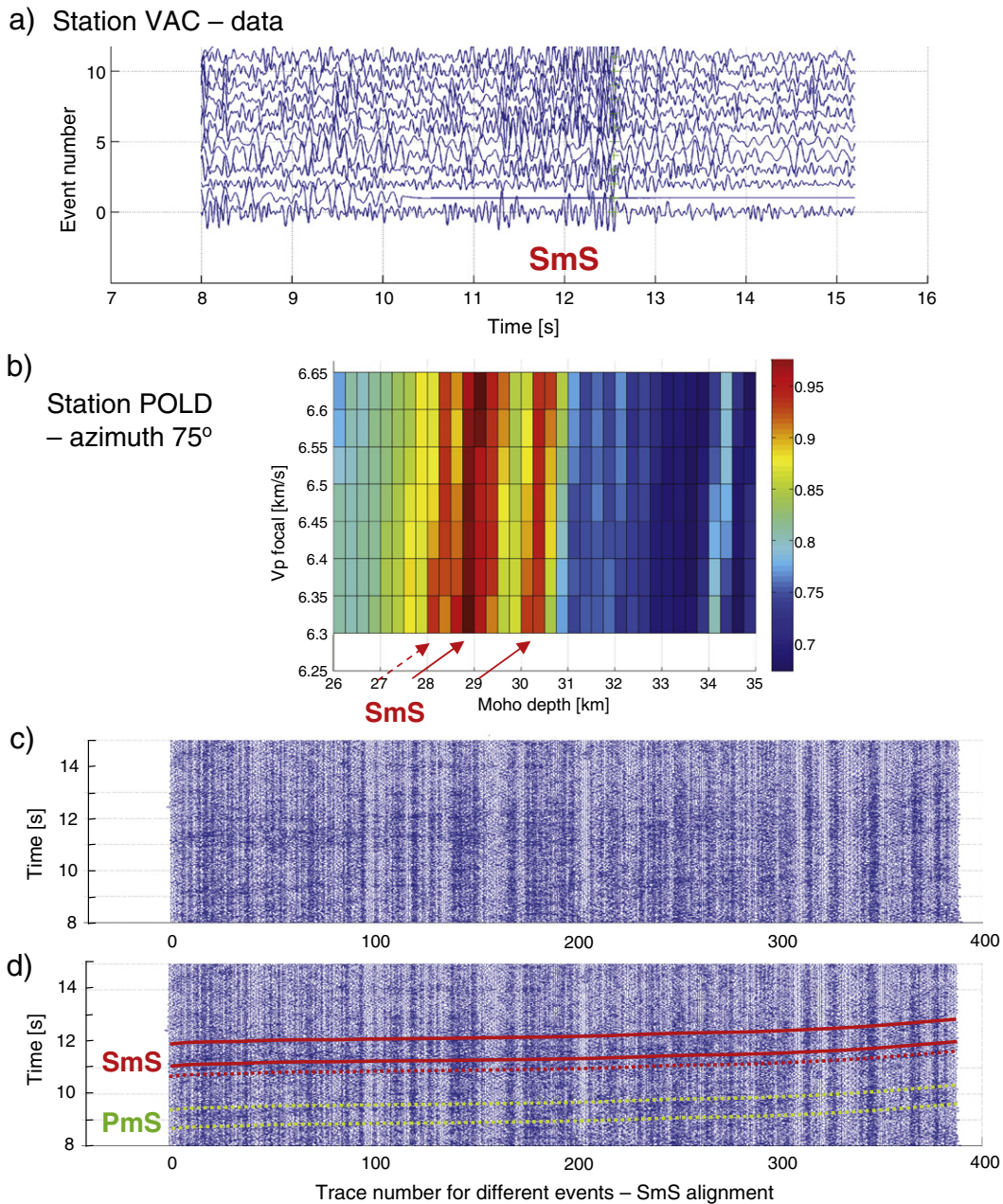


**Fig. 4.** (a) Detailed view of the horizontal velocity records at station VAC aligned and rotated into the optimum azimuth with maximum energy for the Moho reflected *SmS* phase. Note a reflective zone instead of sharp Moho reflections in time of 11.3–12.5 s. (b–d) Inversion of the *SmS* reflections for the Moho depth at station POLD using horizontal velocity records rotated into the optimum azimuth of 75°. (b) Stacked and inverted *SmS* phases with the grid search algorithm. The scale of the plot is normalized to the maximum amplitude of the stack; high values of the stack indicate strongly reflecting interface. The inversion reveals Moho reflections at the depths of ~28.0, 29.0 and 30.5 km, which correspond to the zone of an increased reflectivity in times between about 11 and 12 s. (c) Moho reflected *SmS* phases in the data with a wide reflective zone instead of a single sharp contrast at the Moho. (d) Moho reflected *SmS* phases in the data with travel time curves calculated using ray tracing (red lines). Note Moho converted *PmS* phases indicated for the two most pronounced interfaces at the depths of 29.0 and 30.5 km (green lines).

earthquake region, but with no or only weak imprint on the 410 km discontinuity.

Further, another information about the Quaternary upper mantle processes in West Bohemia/Vogtland was obtained from xenoliths and mega-xenocrysts that were found in a tephra deposit (age: 0.29 Ma; Mrlina et al., 2007) close to the Mýtina maar (Geissler et al., 2007). Xenoliths represent a part of the Earth's lower crust or upper mantle, which has been incorporated into a rising volcanic melt and then subsequently erupted onto the surface. All xenolith and mega-xenocryst samples show a cumulus texture and contain several percent of open pore-space, partly filled with glass (Geissler et al., 2007). The petrographic, geochemical, and thermo-barometric results indicate a lithospheric mantle strongly altered by magmatic processes, which can

result in a decrease of seismic velocities in the uppermost mantle. The depths of origin is estimated to about 25 to 40 km, which might be the intrusion level for the alkaline melts in the past and also at present, since there are still exhalations of gases with upper-mantle isotope signatures (C, He, N) at the surface (Bräuer et al., 2005). Calculated equilibrium or crystallization temperatures are higher than indicated by the extrapolation of regional geotherms derived from surface heat flow studies. Hornblende and clinopyroxene samples could be the fragments of small magmatic intrusions into the uppermost mantle and lower crust (veins, dikes, sills), which could have caused a local-scale, thermal and magmatic overprinting of the Moho, as indicated previously by the receiver function study (Geissler et al., 2005). Lower crustal reflectivity or laminated structure at the Moho level modeled

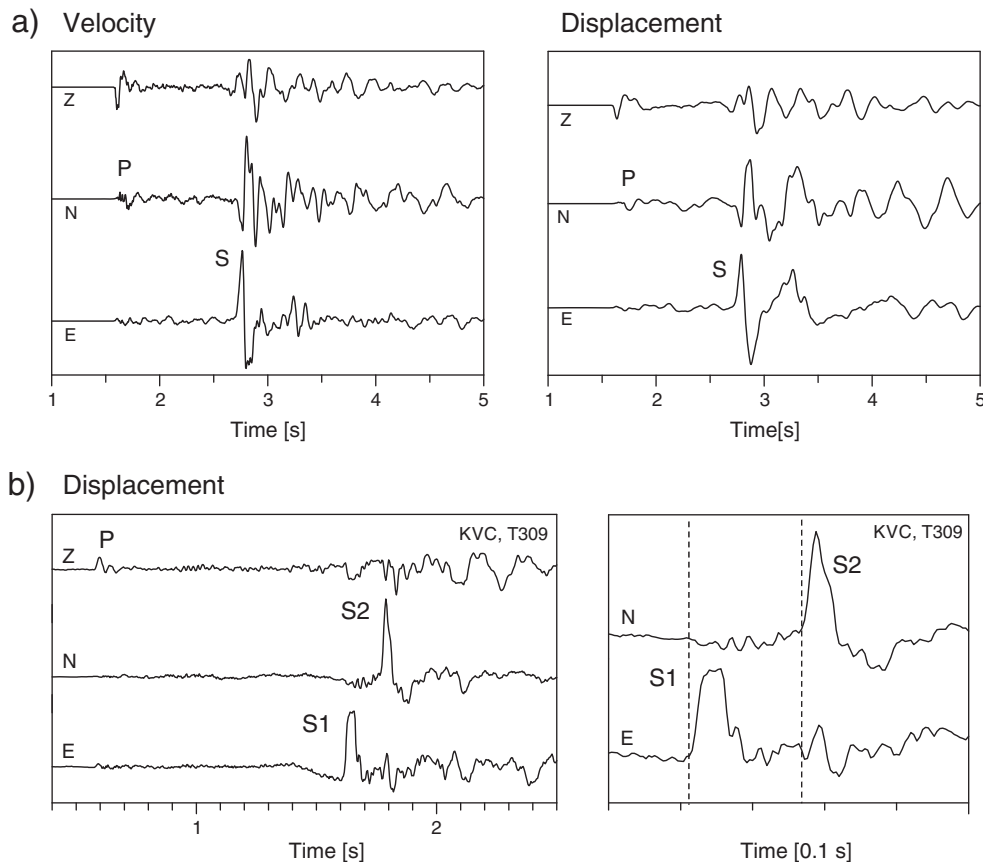


**Fig. 5.** Typical three-component seismograms of swarm earthquakes in West-Bohemia/Vogtland. (a) Velocity and displacement records of  $M_L$  3.7 earthquake of 14 October 2008 at 19:00:33 observed at station NKC. (b) Displacement record of  $M_L$  0.4 microearthquake of December 30, 2001 at 04:00:58 observed at station KVC. A detail (right) of the horizontal S-wave traces showing a strong S-wave splitting that is by coincidence aligned in the geographic directions. The vertical dashed lines mark the arrivals of the split S waves.

by Hrubcová et al. (2005) and Hrubcová et al. (2013) may be explained in a similar way.

### 3.5. Summary

Crustal and upper mantle structure was investigated from several active seismic experiments and passive monitoring. The upper crust exhibits complex structure; shear-wave splitting analysis indicates anisotropic pattern with the overall anisotropy of 4–6%, which can locally reach values up to 10–15%. This implies complicated upper crust composed of diverse geological blocks with different types of anisotropic rocks. Lower crust and crust–mantle transition reveals laminated structure with increased reflectivity, which can be explained by presence of densely spaced thin layers of high and low velocities with the top at the depth of 27–28 km. This can be represented, for example, by alternating mafic/ultramafic material, melt or material with different metamorphic grade. Small magmatic intrusions into the uppermost mantle and lower crust (veins, dikes, sills) could have caused a local-scale, thermal and magmatic overprinting of the Moho. Studies of mantle xenoliths found in 0.29 Ma old tephra deposit indicate depths of their origin at about 25 to 40 km, which might be the intrusion level for the melt in the past.

## 4. Earthquake swarms

Earthquake swarms are usually considered as sequences of numerous small events at shallow focal depths, which cluster in time and space. Few dominant earthquakes (mainshocks) that reach similar magnitudes occur during the course of the earthquake sequence so that smaller events are not associated with any identifiable mainshock.

This is explained as a consequence of a very heterogeneous stress field and/or a weakened crust, which lacks a single well-developed fault and is incapable of sustaining higher strain (Mogi, 1963). Earthquake swarms usually occur in volcanic areas, geothermal fields and ocean ridges (e.g. Dregger et al., 2000; Lees, 1998; Wyss et al., 1997). Intraplate earthquake swarms without active volcanism occur in continental rifts like Rio Grande, Kenya and West Bohemia (Ibs-von Seht et al., 2008). In these places, the occurrence of earthquake swarms is restricted to deep-reaching zones of weakness that allow intrusion of upper mantle material into crustal layers, which seem to be associated with the generation of earthquake swarms.

### 4.1. Swarm observations in the past

Seismic activity in the West Bohemia/Vogtland region (Fig. 4) lies in the southern part of the north–south trending Regensburg–Leipzig seismoactive zone (Bankwitz et al., 2003; Korn et al., 2008). The earthquake observations in West Bohemia/Vogtland date back to the medieval times; however, on the basis of macroseismic data, earthquake swarms have been well documented since the beginning of the 19th century. Credner (1876), who described the earthquakes in 1875, is probably the first who used in literature the term “Erdbebenschwarm” (earthquake swarm). The oldest activity analyzed is the series of more than 100 macroseismically felt earthquakes in 1824 by Knett (1899). A significant increase of earthquake activity was observed at the turn of the 20th century when several stronger swarms were observed by the population. There were the earthquake swarms of 1897, 1900, 1903, and 1908 with approximate maximum intensity  $I_0$  estimates of 6.5, 5.5, 6.5, and 7.0, respectively (Leydecker, 2011). The only historical swarm with seismograph records of sufficient quality is that of 1908,



with the strongest macroseismic observations. Taking the estimate of its maximum magnitude of 4.4 (Neunhöfer and Hemmann, 2005) one arrives at the conclusion that the magnitude of the swarms at the turn of 20th century did not exceed the level of 4.5.

At the beginning of the 20th century the earthquake swarm phenomenon became a subject of popular scientific publications, too. The national history brochure of Kraslice/Graslitz municipality (Treixler, 1929) reports the frequent occurrence of earthquakes since 1824 and also mentions that “from time immemorial no severe damage was ever caused by earthquakes in this region”, which gives indirect verification of our estimate of the level of magnitudes not exceeding  $M_L$  4.5. Interestingly, Kafka (1909) distinguishes between small events that are manifested as underground rumbling and larger events that caused ground shaking during the 1900 swarm in Kraslice.

#### 4.2. Instrumentally recorded swarm activity

The instrumental observations started in 1903 when seismic stations were established in Leipzig, Moxa, and Göttingen. Thus, the investigations of Etzold (1919) represent the first improvement in monitoring with application of instrumental records. In 1962, microseismic monitoring started in the Vogtland area (Neunhöfer, 1976). Significant enhancement of seismic recording arrived when the first local three-component digital seismic stations VAC and TIS were installed during the 1985/86 swarm (Vavryčuk, 1993), and then by installing the NKC station in 1989, which became the core of the WEBNET network set up in 1994 (Horálek et al., 1996). At present, WEBNET consists of 13 permanent and 10 temporary short-period and broadband stations (Fischer et al., 2010) with the magnitude of completeness of  $-0.5$  (Fischer and Bachura, accepted for publication). In the period from 1991 to 2008, the Kraslice Network was operating (Nehybka and Skácelová, 1995), as well. The broader seismogenic region is monitored by the Saxonian Network SXNET (Korn et al., 2008) and the Bavarian Seismological Network (<http://www.erdbeben-in-bayern.de>). Temporary microarray monitoring of the 2008 swarm was carried out, too (Hiemer et al., 2011). The seismograms of the swarm earthquakes are typified by simple waveforms with sharp P and S-wave onsets (Fig. 5).

The present seismicity in West Bohemia and Vogtland is roughly delimited by the area between  $49.9^\circ$  and  $51^\circ$ N and  $12.0^\circ$  and  $12.8^\circ$ E and is strongly clustered, both in space and time. Fischer and Horálek (2003) discriminated the earthquake swarms and solitary events by detecting local minima of the inter-event time series. Beside three major swarms (1985/86, 1997, and 2000), they identified 27 microswarms with magnitudes below  $M_L$  2. Earthquake swarms usually consist of several thousands of earthquakes mostly of  $M_L < 4.0$ . Neunhöfer and Hemmann (2005) applied a classification of the space and time proximity of hypocenters and distinguished the earthquake clusters from solitary events. Earthquake clusters consist of the earthquake swarms and low b-value clusters, which resemble mainshock–aftershock series and belong, together with solitary events, to non-swarms. In total, 121 clusters in the period of 1903–1999 were detected using the database Vocatus (Neunhöfer, 1998) that includes more than 18,000 earthquakes, which occurred during the 20th century. It summarizes the earthquakes monitored in Vogtland since 1962 with local stations within a 100 km epicentral distance and also a small amount of data from strong earthquakes since 1908.

The character of seismic activity varies along the Regensburg–Leipzig zone. While in the south, swarm-like seismicity prevails, the northern part near Plauen, Zwickau, Gera, and Leipzig is typified by rare, solitary events with magnitudes up to 5 (Leydecker, 2011). Hereinafter, we focus our analysis on the West Bohemia/Vogtland, for which a complete seismic dataset is available thanks to more than 20 years of continuous high sensitivity seismic monitoring. Besides, it is a place of  $\text{CO}_2$  degassing and other manifestations of present geodynamic activity.

Fig. 6 shows epicenters of 6700 events ( $M_L > 0.5$ ) from the period of 1991–2012 localized with the velocity model of Málek et al. (2005). Prevailing focal depths are between 6 and 15 km with rare occurrence of foci down to a depth of 25 km (Horálek and Fischer, 2010). Recently derived 3-D tomography velocity model (Růžek and Horálek, 2013) provides similar hypocenter distributions with focal depths that are approximately 1 km shallower. The seismic activity is scattered within an area of about 3500 km<sup>2</sup> and several focal zones can be easily distinguished. Horálek et al. (2000) delineated 7 focal zones and a similar classification is also used in Fig. 6 showing epicenters for the period of 1991–2012. Among the focal zones, the area close to the village of Nový Kostel (NK) dominates with more than 80% of the released seismic moment (Fischer and Michálek, 2008). The activity of individual focal zones is quantified in Fig. 7, which shows the cumulative seismic moment and the monthly seismic moment rate for the NK and other focal zones for the whole investigated period, and proves the dominating role of NK. Additionally, a strong episodic character of the activity is apparent in the whole area – note the stepwise moment release during the swarms. However, the stable range of seismic moment rate ( $10^{12}$ – $10^{14}$  Nm per month) in the inter-swarm period documents lasting seismic activity in the form of solitary events and microswarms.

#### 4.3. Earthquake swarms in the Nový Kostel focal zone

The NK focal zone is formed by a narrow NNW striking belt of about  $12 \times 2$  km, where five  $M_L$  3+ swarms occurred within the past 30 years. There were the swarms in 1985/86 ( $M_L$  4.6), in January 1997 ( $M_L$  2.9), in August–December 2000 ( $M_L$  3.3), in October–November 2008 ( $M_L$  3.8), and in August–September 2011 ( $M_L$  3.5).

The geometry of the NK focal zone has been analyzed first by absolute location methods (Vavryčuk, 1993) and later by more accurate master-event or double-difference method using precise P and S-arrival time picks (Fischer and Horálek, 2003, 2005; Fischer and Michálek, 2008; Horálek and Fischer, 2010; Bouchaala et al., 2013). More than 18,000 events that occurred in the NK focal zone have been relocated for the period of 1991–2012. According to Fischer et al. (2010) and Horálek and Fischer (2010) and the new analysis of the 2011 swarm presented in framework of this study, the seismicity pattern of the NK zone shows the following important features (Fig. 8):

- The hypocenter depths range between 6.5 and 11 km with some clusters down to 13 km. Two sub-clusters, the northern and the southern one are distinguishable. The 2000 and 2008 swarms were located in the southern sub-cluster, while the 1997 and 2011 swarms took place in the northern sub-cluster. A narrow linear zone of hypocenters, which was the place of the onset of the 2011 swarm bridges a prominent seismicity gap between the two sub-clusters. The so-far largest 1985/86 swarm activated both sub-clusters, as visible from the occurrence of the 144 hypocenters (violet diamonds in Fig. 8) relocated by Fischer and Horálek (2003).
- The belt of hypocenters strikes NNW ( $169^\circ$ ) and most of the hypocenters delineate a fault zone steeply dipping ( $70^\circ$ – $80^\circ$ ) to west. This holds mainly for the southern sub-cluster where the 2000 and 2008 earthquake swarms took place. The northern sub-cluster shows a wedge-like shape with the shallower part above  $\sim 8.2$  km dipping west and deeper part dipping east (Fig. 8).
- The five swarms that occurred in NK show diverse evolution and rate of the energy release as well as the duration of the swarm activity. In particular, the recent largest swarms of 2000, 2008, and 2011 show progressively increasing speed of seismic moment release. The approximate duration of the main swarm period, being characterized by occurrence of  $M_L$  2.5+ events, is about 7 weeks for the 1985/1986 swarm, 10 weeks for the 2000 swarm, 4 weeks for the 2008 swarm, and only 2 weeks for the 2011 swarm (Fig. 9).

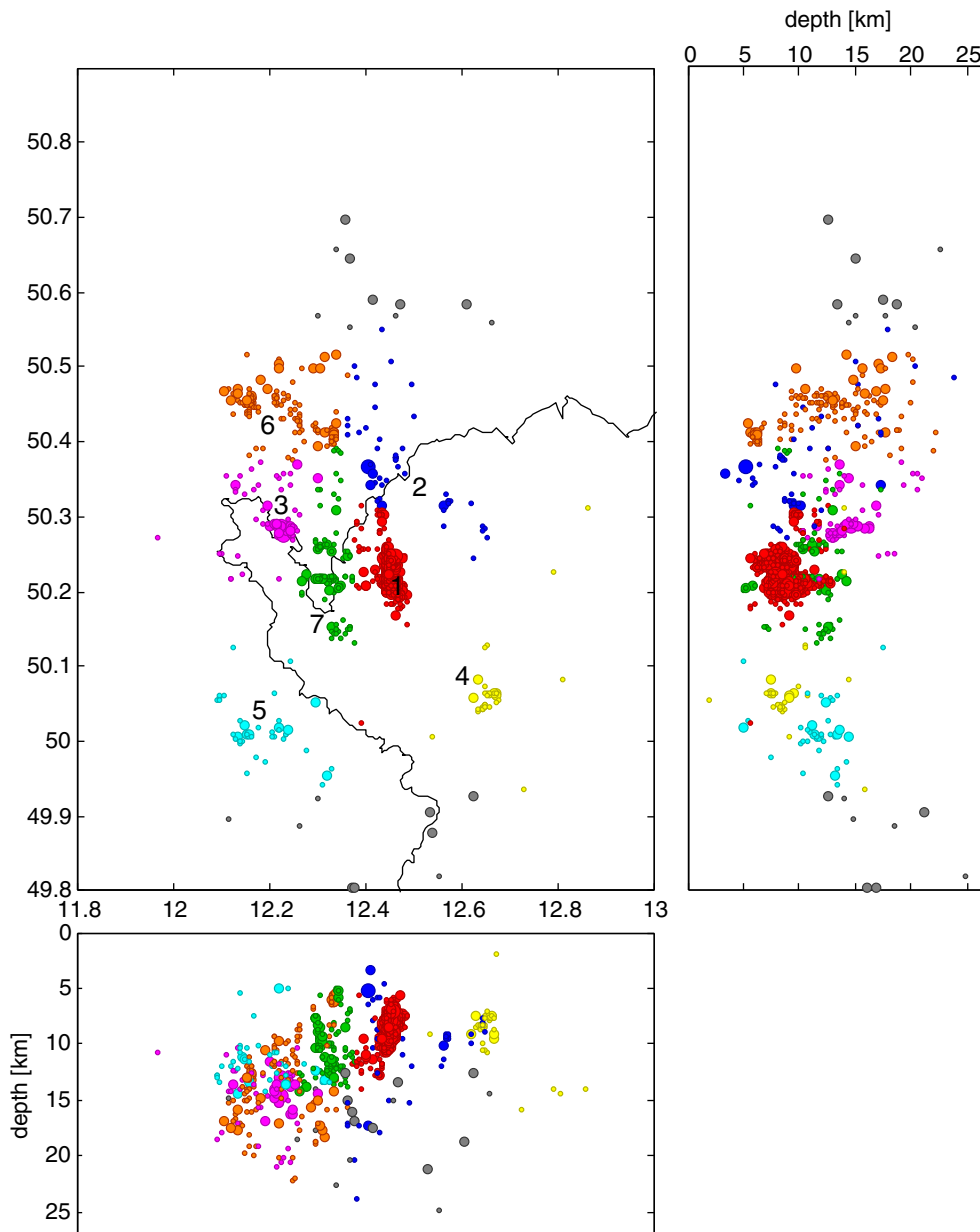


**Fig. 6.** Hypocenters in the West-Bohemia/Vogtland region from the period of 1991–2012. Individual focal zones are indicated by colors (1 – Nový Kostel (NK), 2 – Klingenthal, 3 – Kopaniny – Adorf, 4 – Lazy, 5 – Marktredwitz, 6 – Schöneck, 7 – Plesná) according to Horálek et al. (2000). Gray epicenters are not associated to any focal zone, size of the circle is proportional to the event magnitude.

- The foci of the 1997 swarm were located at depths between 8.5 and 9.5 km in two rather small divergent segments of about  $700 \times 1000$  m in size, which formed a wedge across the fault plane NK.
- The hypocenters of the 2000 and 2008 swarms fall precisely on the same fault portion of the NK focal zone in a depth interval from 6 to 11 km. The fault planes of these swarms appear identical within the bounds of the location error of about 100 m (Bouchaala et al., 2013; Fischer et al., 2010). Both 2000 and 2008 swarms show an oval main fault segment with diameter of about 5 km with a tail pointing upward and to the north. The 2011 swarm started only 34 months after the 2008 swarm, which was the shortest inter-swarm period. The fault patch activated during the 2011 swarm attaches to the northern edge of the 2008 swarm cluster and shows a wedge-like shape (Fig. 8).
- All the swarms show a strongly episodic character of activity. This was first addressed in detail for the 2000 swarm, which lasted four

months and consisted of nine swarm phases. These episodes persisted couple of days at most and were separated by periods of quiescence (Fischer, 2003). A similar temporal pattern was also observed for the 2008 and 2011 swarms; however, the faster evolution of the activity resulted in overlapping of individual swarm phases, which was especially the case of the 2011 swarm (Fig. 9).

- The inter-swarm activity shows different patterns. While the few-year periods prior to the 2000 and 2011 swarms display scattered seismicity, the longer 8-year period prior to the 2008 swarm was preceded by a sequence of microswarms that initiated in 2004 and showed increasing maximum magnitudes reaching  $M_L \sim 2.0$ .

#### 4.4. Earthquake source studies

Directivity effects of seismic sources were analyzed by Fischer (2005) who used the empirical Green's function (EGF) method to study the seismograms of 80 selected events of the 2000 swarm and

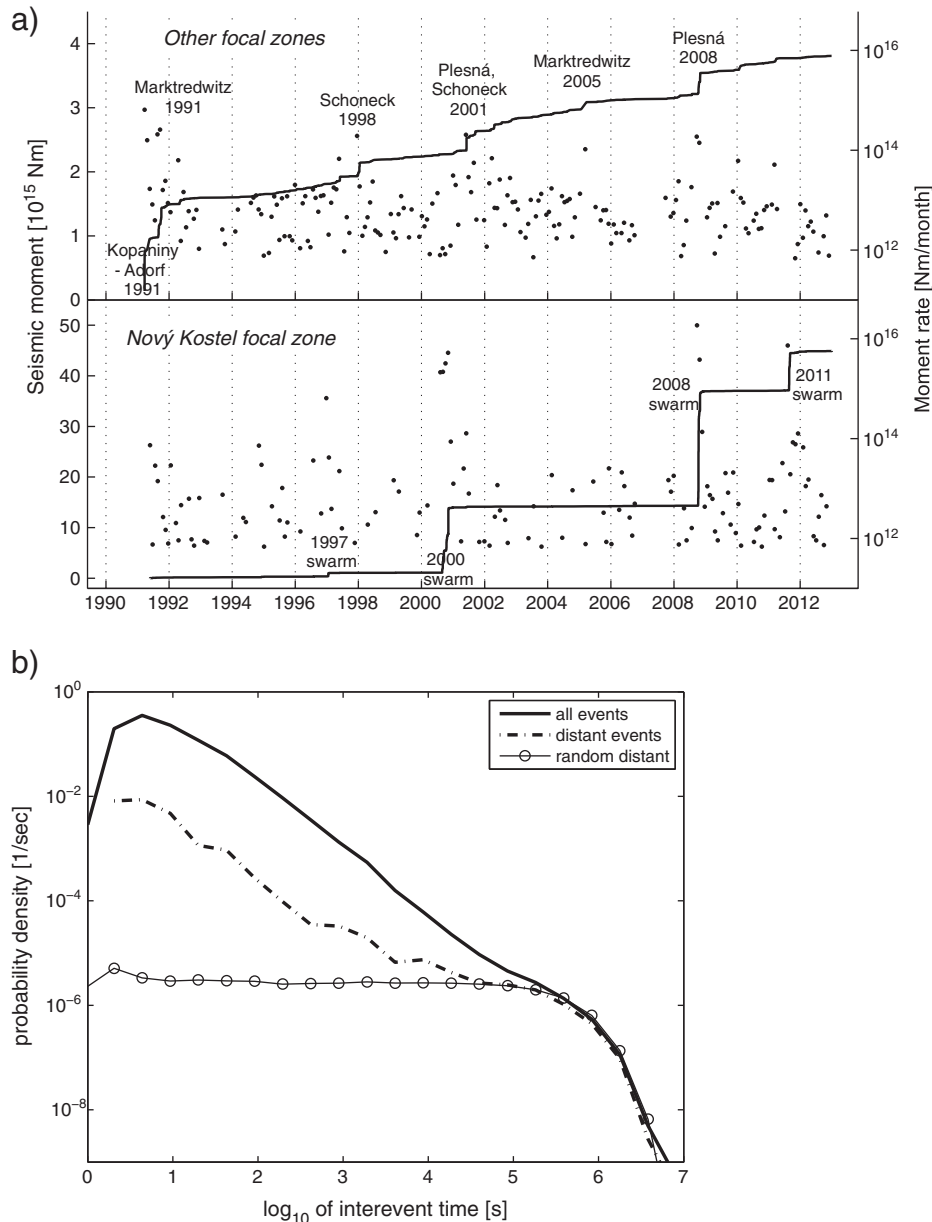


**Fig. 7.** (a) Seismic moment release in the West Bohemia/Vogtland area or the Nový Kostel focal zone (bottom) and for the other focal zones (top); full line: cumulative seismic moment; symbols: monthly moment rate; (b) Probability density function of inter-event times of the earthquakes from the period of 1991–2009 measured among all events (full line), distant events separated by more than 5 km (broken line) and distant events with random origin times (thin line with symbols). Note the power-law dependence for all event pairs and distant event pairs in the interval from about 3 s to about 30 000 s (indicated by vertical dashed lines).

found that many of them display a complex source-time function composed of several pulses. Seismogram modeling revealed that some of these events are generated by a fast stick-slip rupturing composed of several rupture episodes separated in time and space. The relative positions of the sub-events with respect to the orientation of the fault indicate that most of them occurred on a common fault plane. Scaling of the distance with magnitude conforms the average stress drop of about 10 MPa and average rupture velocity of  $3.0 \pm 0.9$  km s<sup>-1</sup>. The stick-slip character of earthquake rupture during the 2000 swarm can be explained by stress and/or structural heterogeneities of the fault zone that impede or arrest the rupture propagation. These heterogeneities thus prevent generation of large events, whose lack is typical for earthquake swarms as reflected in the higher b-values of their magnitude–frequency distribution (Hainzl and Fischer, 2002).

Kolář and Růžek (2012) analyzed stopping phases of 36 events ( $M_L$  1.7–3.0) of the 2000 swarm to determine the source radius and

rupture velocity for circular source model. The results are fairly consistent with a constant stress-drop model with source radii ranging from 120 to 350 m. The typical value of stress drop  $\Delta\sigma = 2.4$  MPa is in a good agreement with  $\Delta\sigma = 1.7$  MPa, given by Hainzl and Fischer (2002), who compared the spatial extent of the swarm 2000 activity with the total released seismic moment. However, Michálek and Fischer (2013) determined the static source parameters of 60  $M_L < 3.0$  earthquakes of the 2000 and 2008 swarms and found quite high stress drop that varied between 0.6 and 60 MPa in terms of the Brune's model. The non-self similarity of earthquakes stems both from an overall increase of stress drop with seismic moment and is also manifested in similar corner frequency for events that differ by more than one magnitude level.

Vavryčuk (2011c) studied source-time functions of 12 selected events of magnitudes between 1.7 and 3.7 that occurred in the 2008 swarm. The analysis reveals that the focal mechanisms are frequency



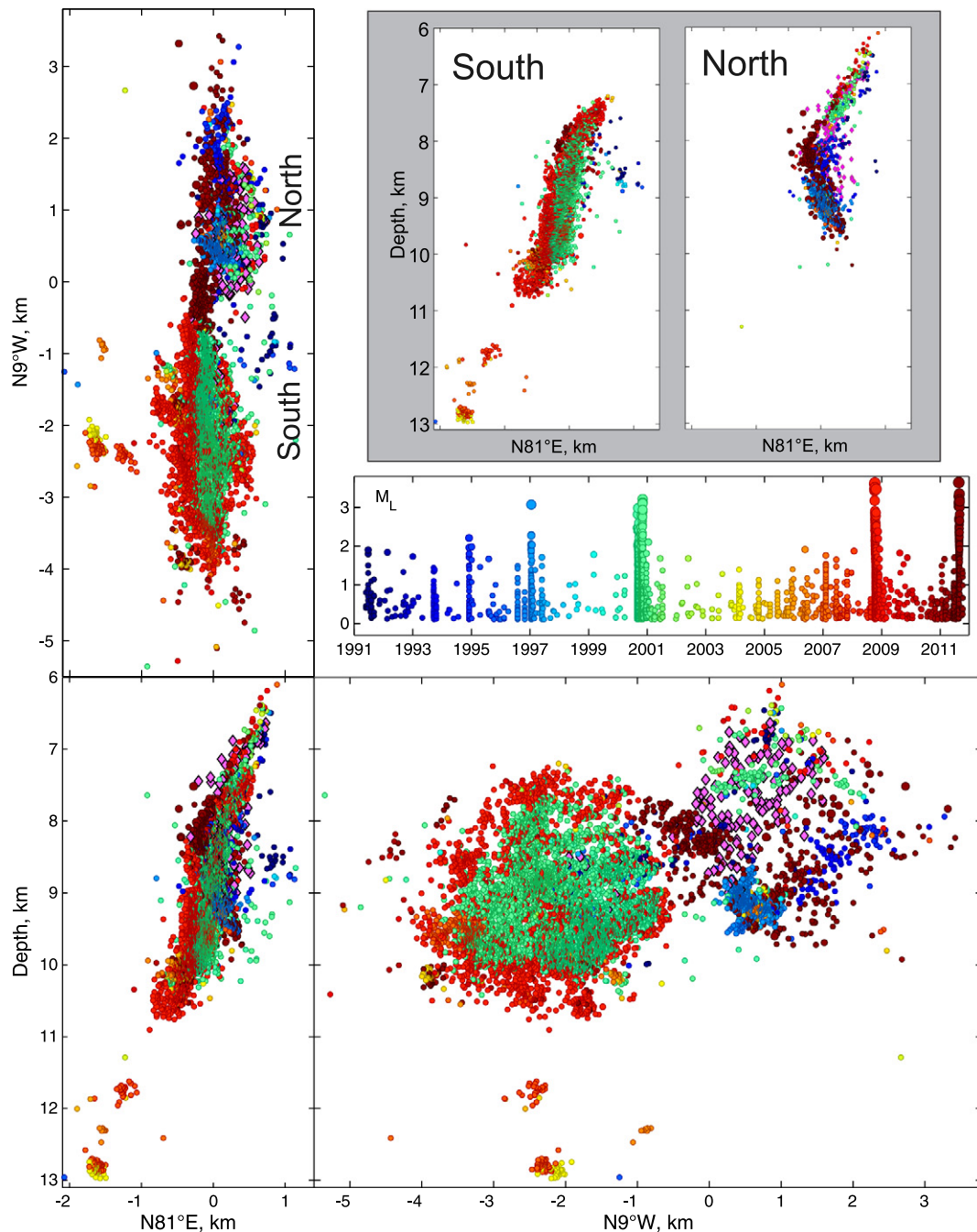


**Fig. 8.** Hypocenters of the earthquakes occurred in the Nový Kostel focal zone (NK) in the period 1991–2011 (color proportional to time) and the 1985/86 swarm (violet diamonds) obtained by the master-event location method with the relative location error below 100 m. Map view (top-left), two perpendicular sections (bottom), magnitude–time plot (middle-right) and sections of the southern and northern cluster (top-right) are shown. The symbol size is proportional to event magnitude. For the 1985/86 swarm only the period Jan–Feb 1986, that occurred mostly in the northern cluster is displayed.

dependent: the source–time function in the low-frequency band is mainly produced by shear rupturing along a fault while the high frequencies in the source–time function are produced by some other mechanism, probably by weak tensile vibrations of the fault. The vibrations seem to be of a narrow frequency band with frequencies distinctly higher than those of shear rupturing. They complicate the radiated P waveforms and the P-wave radiation pattern. The tensile vibrations can be observed in waveforms in directions near the nodal lines where the dominance of shear-faulting radiation is lost. The tensile vibrations could be generated, for example, by opening of the fault activated during shear rupturing or by creating a wing tensile crack at the tip of the fault when shear fracturing stops.

#### 4.5. Summary

The earthquake swarms in West Bohemia/Vogtland have already been observed in historic records; the magnitude of the strongest earthquakes in the documented seismic crises in 1824, 1897–1908, and 1985–2011 did not exceed  $M_L$  4.5. The activity in the area close to Nový Kostel stands out during the recent seismic period where hypocenters cluster at depths from 6 to 13 km along a steeply dipping fault plane with complicated geometry and the width below 100 m. These earthquake swarms show strongly episodic character of activity and migration of hypocenters. A reactivation of previously ruptured areas is frequently observed.

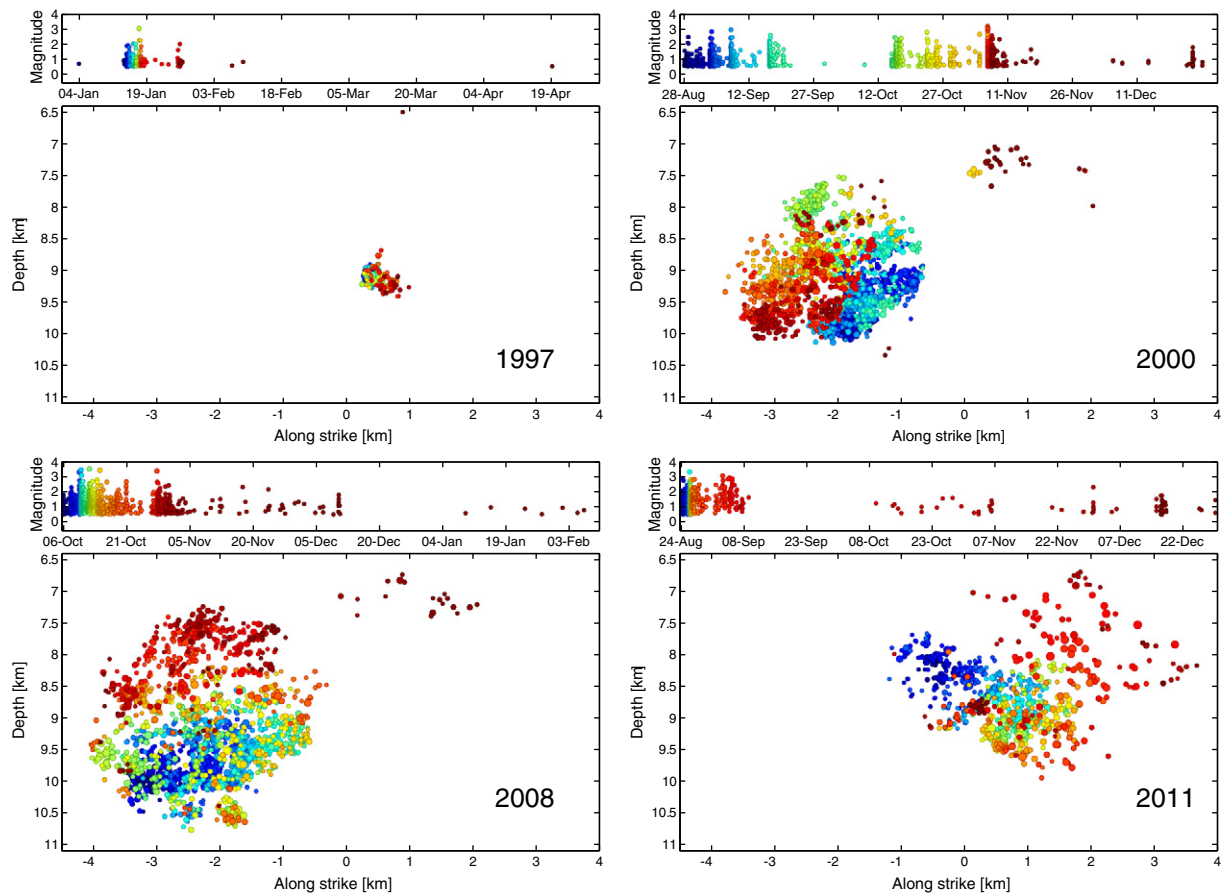


**Fig. 9.** The 1997, 2000, 2008 and 2011 swarm activity in the magnitude–time plot (top) and fault plane view (bottom) (the same projection as the lower right view in Fig. 8). Color-coding denotes the event order in time. Note that (i) despite the similar duration of the 1997 and 2011 swarm activities, the activated focal area is much larger for the 2011 swarm; (ii) the 2000 and 2008 swarms initiated at the bottom of the fault patch (dark-blue colors) and terminated at the top-most tail on the right. In contrast, the 2011 swarm has initiated at the top-northern corner of the 2008-swarm fault patch. Similar time period of 128 days is displayed for all three swarms.

## 5. Earthquake source mechanisms and stress field

### 5.1. Focal mechanisms and their occurrence during swarms

Complexity of the focal zone and the orientation of active fault systems in the area are best studied using focal mechanisms. So far, accurate and reliable focal mechanisms were calculated for earthquakes of several prominent earthquake swarms in the Nový Kostel area in the period from 1985 to 2011. Focal mechanisms of several strongest earthquakes of the 1985/86 swarm were obtained by Antonini (1988) and Špičák (1987) using P-wave polarities. Dahm et al. (2000) selected 70 earthquakes of the 1997 swarm and calculated full moment tensors from direct P- and SH-wave amplitudes measured manually in the three-component ground displacement seismograms and using single- and multiple-source moment tensor inversions. Full moment tensors were retrieved and interpreted for the same data also by Horálek et al. (2002). Fischer and Horálek (2005) calculated focal mechanisms of 133 earthquakes of the 2000 swarm with magnitudes  $M_L > 1.7$  using the P-wave polarities and the S/P amplitude ratios. Additionally, the full moment tensors of the 2000 swarm were determined by Horálek and Šílený (2013) for 102 selected earthquakes applying the same method as in Horálek et al. (2002).

As the quality and amount of seismic observations gradually increased with time, the best accuracy of source mechanisms was achieved for recent swarms. This is the case of source mechanisms of 99 earthquakes of the 2008 swarm (Vavryčuk, 2011a) and a detailed study of the foci clustering and the corresponding focal mechanisms for 250 earthquakes of the 2008 swarm as presented by Vavryčuk

et al. (2013). Besides the focal mechanisms, also the occurrence of double-couple and non-double couple components of the full moment tensors was studied for selected earthquakes of the 1997, 2000, and 2008 swarms (Horálek and Šílený, 2013; Horálek et al., 2002; Vavryčuk, 2002, 2011b) as discussed in Section 5.4.

The results of the focal mechanism studies show that the prevailing focal mechanisms in the Nový Kostel zone have strikes in the range of  $165\text{--}180^\circ$ , which reflect the predominant orientation of the focal zone coinciding with the N–S direction of the PPZ. For example, the strongest event of the 1985/86 swarm with  $M_L = 4.6$ , which occurred on December 21, 1985 at 10:16, with strike of  $171^\circ$ , dip of  $75^\circ$  and rake of  $-30^\circ$  (Fig. 10a), belongs to this group (Antonini, 1988; Zahradník et al., 1990). Similar mechanisms are very frequent and occur also in other swarm activities in 2000 (Fig. 10a), 2008 (Fig. 10a, red nodal lines) and 2011. Other focal mechanisms are also present in the area but they are minor. The exception was the 1997 swarm (Fig. 10a) represented by two following basic types of the focal mechanisms: the focal mechanism with strikes in the range of  $300\text{--}310^\circ$ , and the other with strikes in the range of  $35\text{--}45^\circ$  (Horálek et al., 2002; Vavryčuk, 2002). These focal mechanisms were present also in the 2008 swarm but only exceptionally (Fig. 10a, blue nodal lines).

### 5.2. Detailed geometry of the Nový Kostel focal zone

Bouchaala et al. (2013) applied the double-difference approach to relocate 483 selected events of the 2008 swarm and to reveal the fine geometry of the fault surface. The mean location error has

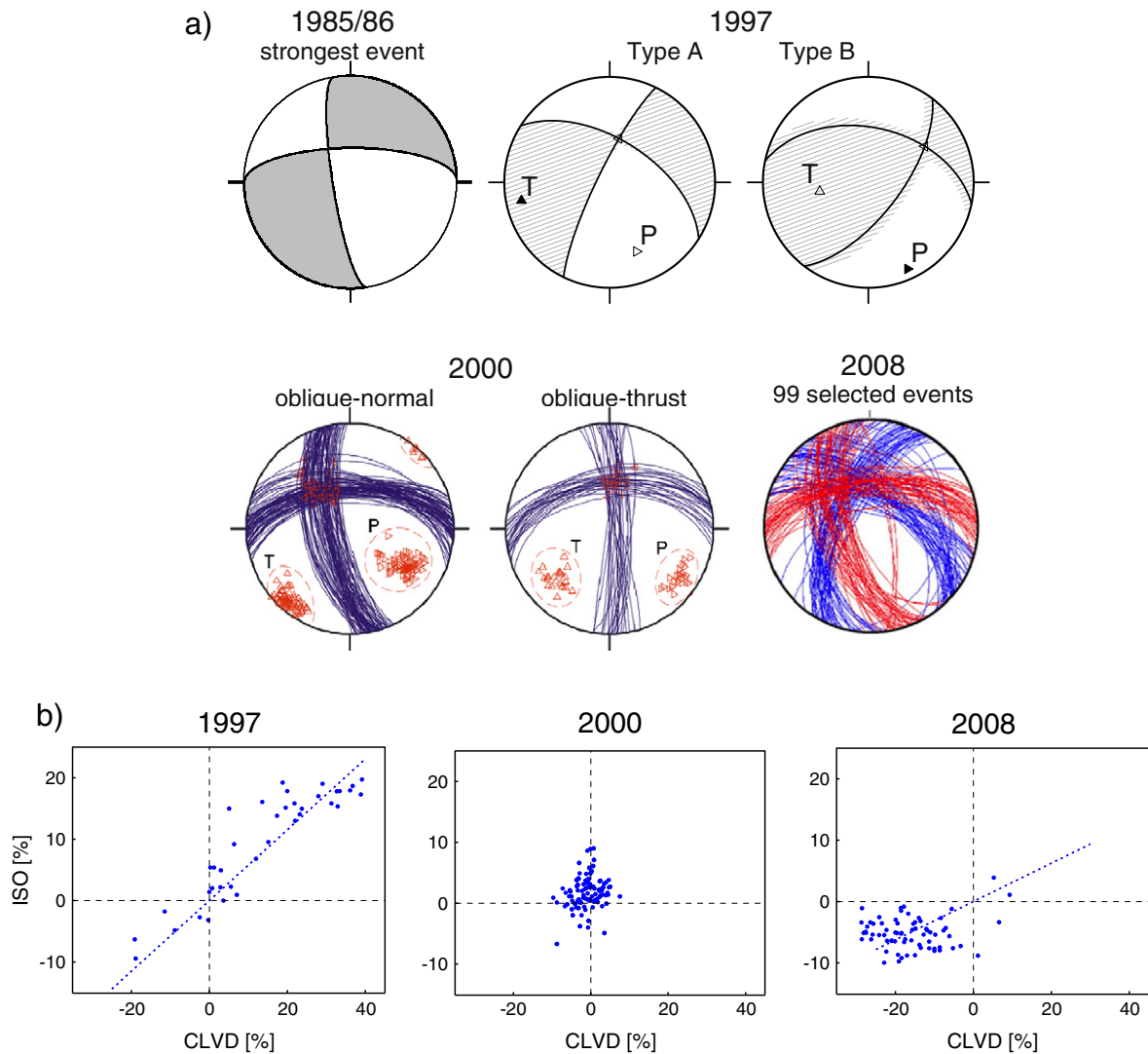


**Fig. 10.** (a) Focal mechanisms of earthquake swarms in the NK zone: Strongest  $M_L = 4.6$  event of the 1985/86 swarm (from Antonini, 1988); type A and B events of the 1997 swarm (Horálek et al., 2002); right-lateral (in blue) and left-lateral (in red) events of the 2008 swarm (Vavryčuk, 2011a); the right-lateral events were exceptional only. (b) Non-double-couple components of the moment tensors of the 1997, 2000 and 2008 swarms (Vavryčuk, 2011b; Horálek and Šílený, 2013).

dropped from 62 m for the master event method to 17 m for the double-difference method using the cross-correlation delay measurements. A more focused fault image was obtained; however, the improvement was not very significant, which points to a good quality of the master-event locations. Vavryčuk et al. (2013) compared the fault surface geometry with focal mechanisms to find if the rupture of individual events follows the fault surface and if the swarm activity can be interpreted as stick-slip rupture of a single fault plane as suggested by Hainzl and Fischer (2002) for the 2000 swarm. Vavryčuk et al. (2013) revealed that the fault active during the 2008 swarm has a complex geometry being composed of several fault segments with different orientations. Some of the segments intersect each other. The orientations of the segments coincide well with the focal mechanisms (see Fig. 11). Some segments are optimally oriented with respect to tectonic stress in the region (see Section 5.3), but some of them are misoriented. The effective normal traction is small on them and might occasionally become extensive, which would result in tensile opening. This indicates that some microearthquakes occurring in the focal zone should be shear-tensile events, which represent simultaneous shearing and opening with slip vector deviated from the fault plane as described by Vavryčuk (2002, 2011b) and by Fischer and Guest (2011).

### 5.3. Tectonic stress and principal focal mechanisms

Tectonic stress was determined in the West Bohemia region from focal mechanisms by applying the inversion method of Gephart and Forsyth (1984) and its modifications (Angelier, 2002; Lund and Slunga, 1999) using various datasets by Havří (2000), Slancová and Horálek (2000), Vavryčuk (2001, 2002, 2011a), and Plenefisch and Klinge (2003). The stress inversions (Fig. 12) yield the maximum compression direction in the range of 135–155°E inclining from the horizontal plane by 25–45°. The azimuth of the maximum compression  $\sigma_1$  coincides well with the average direction N144°E in Western Europe (Heidbach et al., 2008). The value is slightly rotated with respect to N160°E measured at the KTB superdeep borehole (Brudy et al., 1997), located about 50 km SW of the Nový Kostel zone. Interestingly, the  $\sigma_3$  axis is close to horizontal and the  $\sigma_1$  and  $\sigma_2$  axes deviate from the horizontal plane. No temporal variations of stress orientation were detected because of uncertainties of the stress inversion. Probably, the most representative values of stress were published by Vavryčuk (2011a) who used 99 accurate and carefully selected focal mechanisms to ensure their balanced variety. The inversion yielded for the  $\sigma_1$ ,  $\sigma_2$  and  $\sigma_3$  axes the following angles (azimuth/plunge): 146°/48°, 327°/42° and 237°/1°. The optimum stress shape ratio defined as  $R = (\sigma_1 - \sigma_2)/(\sigma_1 - \sigma_3)$  was 0.8.



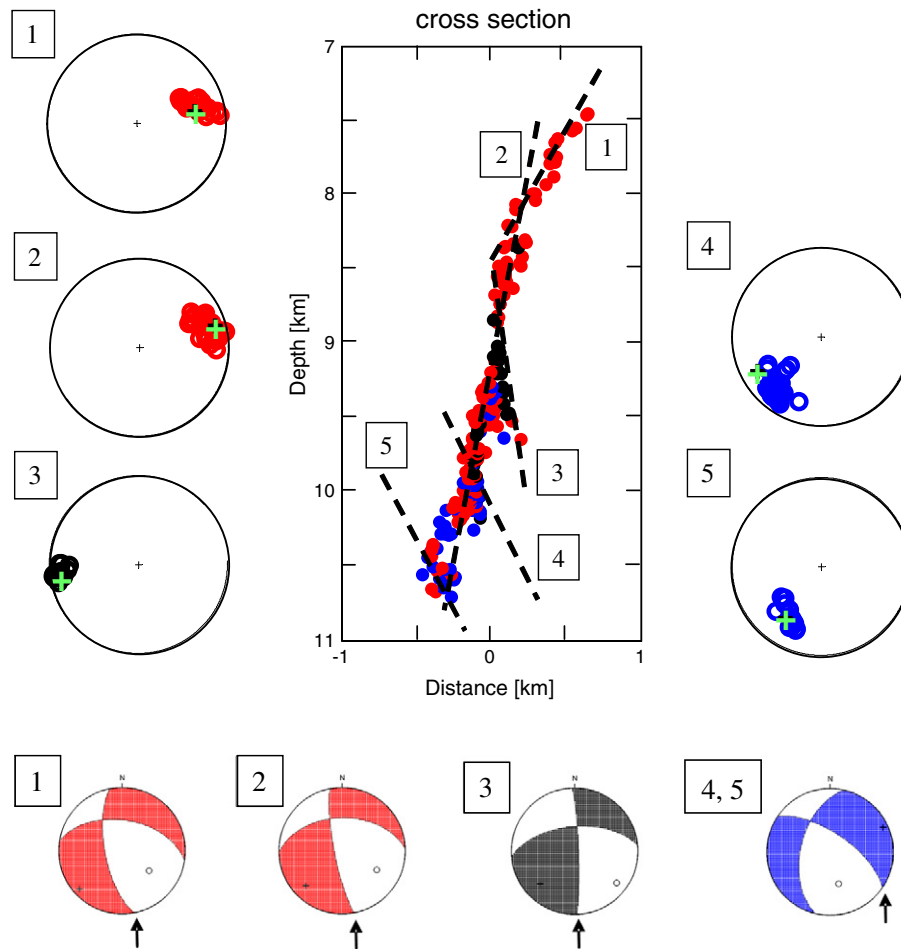


**Fig. 11.** The segmentation of the NK focal area using the plane fitting to foci and the diversity of focal mechanisms of the 2008 swarm earthquakes. The foci and fault normals are color-coded according to their focal mechanism (lower plots). The numbers identify the individual fault segments displaying a uniform focal mechanism. The open circles in the focal spheres show the orientations of the fault normals computed from the focal mechanisms of events belonging to individual fault segments. The green plus signs mark the fault normals computed using the fitting of plane to foci. The lower plots show the typical focal mechanisms with arrows indicating the fault planes.

Knowing the stress field in the region one can analyze stress conditions on active faults and plot their positions in the Mohr's diagram (Fig. 12). The analysis reveals that focal mechanism with strike of  $169^\circ$ , dip of  $68^\circ$ , and rake of  $-44^\circ$  (left-lateral strike slip with a weak normal component), which is the predominant mechanism in the area, and the focal mechanism with strike of  $304^\circ$ , dip of  $66^\circ$ , and rake of  $-137^\circ$  (right-lateral strike slip with a weak normal component) belong to a pair of conjugate principal faults (Fig. 13). These faults are most unstable being optimally oriented for shearing under the present tectonic stress (Vavryčuk, 2011a). The left-lateral strike-slip fault is identified with the PPZ fault, which is parallel to the Nový Kostel focal zone, and the right-lateral strike slip fault corresponds to a slightly rotated branch of the MLF. The other focal mechanisms such as those observed during the 1997 swarm with strikes in a range of  $35\text{--}45^\circ$  (events B in Fig. 10a and type 3 events in Fig. 11) occurred on faults which are misoriented with respect to the tectonic stress. If the normal traction on these fault planes becomes negative, significant non-shear (non-double-couple) components in the moment tensors can be generated (Fischer and Guest, 2011).

#### 5.4. Non-double-couple components and their origin

The analysis of the non-double-couple components of moment tensors in the 1997, 2000 and 2008 swarms reveals that the amount of non-double-couple components varies significantly (Fig. 10b) and is basically determined by the orientation of the fault in the tectonic stress

field. The moment tensors of earthquakes, which occurred on the optimally oriented principal faults (most of the events in the 2000 and 2008 swarms) are mostly shear as shown by Horálek and Šílený (2013) for the 2000 swarm. However, the moment tensors of the 2008 swarm determined by Vavryčuk (2011b) show small compressive isotropic (ISO) and compensated linear vector dipole (CLVD) components. The origin of this discrepancy will be a subject of further research. In contrast, the moment tensors of earthquakes occurring on the misoriented faults (most of the 1997 swarm events) are characterized by significant positive ISO and CLVD components (Horálek et al., 2002; Vavryčuk, 2002). The presence of the non-double-couple components, whose amount seems to be independent of earthquake magnitude, can be explained by high pore pressure due to the presence of fluids in the focal zone. As an example, this was the case of the B type events that occurred in the second half of the 1997 swarm. By analyzing the moment tensors of the 1997 swarm and the corresponding fault tractions (Fig. 12b), the fluid pressure was estimated to be less than the lithostatic stress only by about 5 MPa (Vavryčuk, 2002).

As mentioned in Section 4.4, significant non-double-couple components are also observed if only high-frequency part of the wavefield is inverted for the moment tensor and for the source-time function. The source process in the high-frequency band contains generally more non-double-couple components which can reflect either small-scale complexities in fault geometry, tensile vibrations of the fault or subsequent rupturing of wing cracks at tips of the fault (Vavryčuk, 2011c).

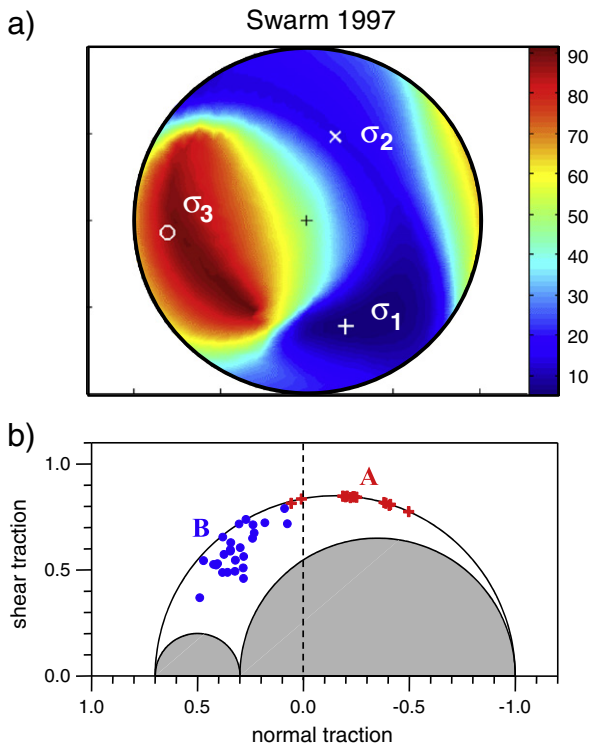


**Fig. 12.** (a) Inversion for stress for the 1997 swarm using the method of Gephart and Forsyth (1984). The misfit function for the  $\sigma_1$  direction (average of deviations between the slip and shear traction direction on the fault measured in degrees) is displayed for the whole lower hemisphere. The equal-area projection is used. (b) Mohr's circle diagram for the type A (red plus signs) and type B (blue dots) earthquakes (see Fig. 9). All permissible values of shear and normal traction must lie inside the large circle but outside of the smaller circles. The dashed line indicates the zero effective normal traction and separates areas with tensile and compressive stress regimes. After Vavryčuk (2002).

## 5.5. Summary

The prevailing focal mechanisms in the NK focal zone strike about  $170^\circ$ , which is parallel to the orientation of the fault plane delineated by hypocenter clustering. Even the orientation of less frequent conjugate focal mechanisms follows the macroscopic fault plane, which suggests that the individual ruptures represent a step-wise rupturing of a major fault plane accompanied by a system of minor associated faults. The stress field inverted from the focal mechanisms with the azimuth/plunge of maximum compression of  $146^\circ/48^\circ$  is consistent with that of Western Europe. Significant non-double-couple components were found in moment tensors of some earthquakes in the NK zone, which are consistent with shear-tensile character of the ruptures that could be caused by fluid pressure locally exceeding the minimum principal stress. Non-double-couple components are also observed in high-frequency part of radiated waves, which probably reflect small-scale complexities of fault geometry or details in the rupture process.

## 6. Fluids in the lithosphere and the earthquake swarms

Fluids are involved in most active geological processes and their investigations contribute to the understanding of complex geodynamic processes in the Earth's crust and upper mantle. The investigation of gases from  $\text{CO}_2$ -rich mineral springs and mofettes in West Bohemia/Vogtland focuses on the origin of fluids, the evaluation of fluid migration paths and the role of fluids as possible triggering mechanism of the earthquake swarms.

### 6.1. Regional distribution pattern and origin of $\text{CO}_2$ degassing in West Bohemia/Vogtland

The West Bohemia/Vogtland area is known for massive  $\text{CO}_2$  degassing that occurs in the form of  $\text{CO}_2$ -rich mineral waters and wet and dry mofettes in several degassing fields. The total gas flow is more than  $500 \text{ m}^3/\text{h}$  and is mainly concentrated in three degassing centers: (1) Cheb Basin (CB), (2) Mariánské Lázně and its eastern surroundings (ML), and (3) Karlovy Vary (KV) (Geissler et al., 2005; Kämpf et al., 2007; Weinlich et al., 1999; and Fig. 14). These degassing centers are characterized by high gas flow,  $\text{CO}_2$  concentrations of more than 99 vol.%,  $\delta^{13}\text{C}$  values between  $-2$  and  $-4\text{‰}$ , as well as high mantle-derived helium contents. With increasing distance from the degassing centers, the gas flow and  $\text{CO}_2$  contents, as well as both  $\delta^{13}\text{C}$  values and  $^3\text{He}/^4\text{He}$  ratios decrease (Fig. 14).

$\text{CO}_2$  is the carrier phase for mantle-derived minor components like helium whose isotope ratios are the best tool to distinguish crustal or mantle-derived origin of fluids. The gases in West Bohemia/Vogtland have high  $^3\text{He}/^4\text{He}$  ratios; significantly higher than the average continental crust, which is a characteristics indicating their mantle-derived origin. Also, the carbon isotopic studies of  $\delta^{13}\text{C}$  values in the  $\text{CO}_2$ -rich gas escapes indicate the origin in the upper mantle (Bräuer et al., 2004; Weinlich et al., 1999). The highest portions of mantle-derived helium (up to  $6 R_a$ , where  $R_a$  corresponds to the  $^3\text{He}/^4\text{He}$  ratio of the atmosphere) were found in the CB followed by the ML (up to  $4.9 R_a$ ); the KV degassing center has the lowest  $^3\text{He}/^4\text{He}$  ratios ( $2.5 R_a$ ). Lower He-isotope ratios (e.g.  $^3\text{He}/^4\text{He} < 6 R_a$ ) likely reflect mixing with crustal-derived He along fluid pathways (Bräuer et al., 2008).

### 6.2. Possible relation of the fluid signature to seismic and magmatic activity

The first gas-isotope sampling was carried out in 1993 and since 2000 measurements of  $^3\text{He}/^4\text{He}$  ratios and  $\delta^{13}\text{C}$  values are repeated with varying periods. Between May 2000 and December 2003 weekly sampling was carried out at four locations in the Cheb Basin and its periphery, covering also the M<sub>L</sub> 3.2 earthquake swarm of 2000. The degassing centers show different temporal behavior of the  $^3\text{He}/^4\text{He}$  ratios (Bräuer et al., 2009, 2011). While increase in the mantle-helium was observed in CB, the locations near ML keep more or less the same values (e.g. Bräuer et al., 2005). This is attributed to the higher level of seismicity in the area of CB (Nový Kostel focal zone) compared to a weak seismicity in ML (Fig. 15, inset). The progressive increase of the  $^3\text{He}/^4\text{He}$  ratios in the CB degassing center indicates an ongoing hidden magmatic process beneath the CB, which may be responsible for the recurrence of earthquake swarms in the Nový Kostel focal zone (Bräuer et al., 2009).

The observed pre-seismic decrease of  $^3\text{He}/^4\text{He}$  ratios at the Wettingquelle spring and at Bublák during the earthquake swarm of 2000 was interpreted by strain changes of the rock associated with the preparatory phase of the earthquake (Bräuer et al., 2007, 2008). This anomaly correlated with anomalous groundwater level changes in a borehole close to Wettingquelle (Koch et al., 2003).

In contrast to helium that is steadily produced in the crust and may be admixed along the whole migration path, the  $\text{CO}_2$  is trapped in fluid inclusions and can be only released by fracturing. There is a wide range of  $\delta^{13}\text{C}$  values of  $\text{CO}_2$  trapped in fluid inclusions in the crust (e.g. Reutel, 1992) and due to the migration of hypocenters different crustal reservoirs may be opened, which could result in shifts of the  $\delta^{13}\text{C}$  values of the  $\text{CO}_2$  arriving at the degassing site. This co-seismic phenomenon was observed repeatedly after the start of the 2000 swarm, where several swarm phases with migrating hypocenters were distinguished (see Section 7.3). During to the 2000 swarm the first modified  $\text{CO}_2$  in this manner arrived at Wettingquelle mineral spring after about 150 days (Bräuer et al., 2007). This time span is in the same order as that observed after the short swarm of December 4 and 5, 1994 at the neighboring Eisenquelle (Bräuer et al., 2003).

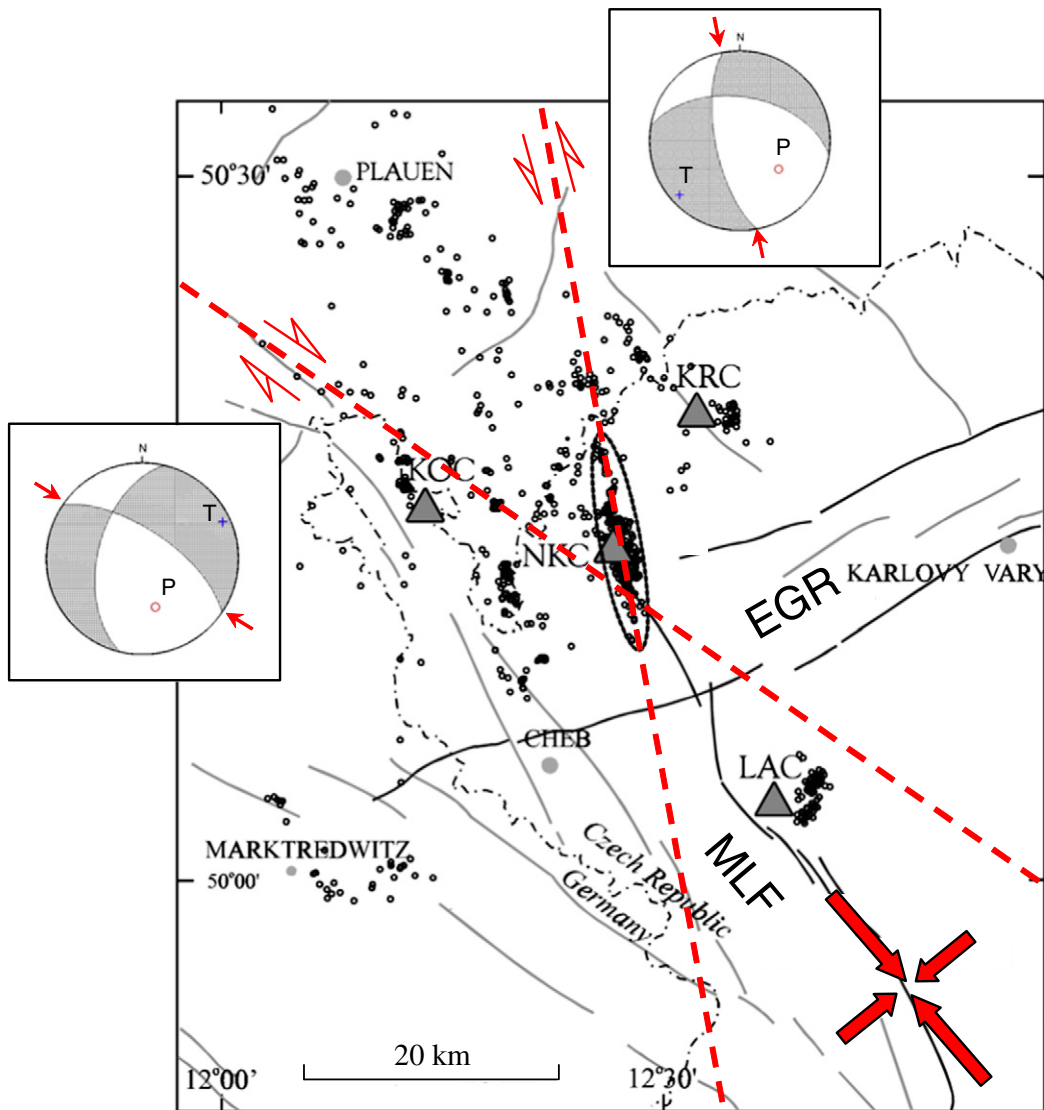


**Fig. 13.** Tectonic sketch of the West Bohemia/Vogtland region. The main fault systems are denoted as MLF (Mariánské-Lázně fault) and EGR (Eger Rift). The gray dots mark the epicenters of micro-earthquakes that occurred in 1991–1999. The 2000 and 2008 swarm epicenters are inside the ellipse, which delineates the most active focal zone in the area (the Nový Kostel zone). The red dashed lines show the orientation of the principal faults found from stress analysis. The full red arrows show the orientation of maximum and minimum compressive stress axes. The two focal mechanisms correspond to the principal faults, the principal fault nodal lines are marked by red arrows. After Vavříček (2011a).

No gas emanations were found at the surface directly above the hypocentral area in the vicinity of Nový Kostel (Fig. 15). Assuming that gas migration paths are subvertical at this part of the crust Bräuer et al. (2003) proposed that low-permeable rock units cap the active hydraulic system and trap the ascending fluids preventing the mantle fluid flow from rising further. This would result in fluid pressure build-up in the surroundings of the focal zone.

### 6.3. Possible relation of groundwater regime and gas flow with seismic activity

Significant changes in mineral spring parameters (water temperature, hydrochemistry) were observed due to the  $M_L$  4.6 earthquake swarm in 1985/1986 at the springs of the spa Františkovy Lázně, and Bad Elster about 15 km and 17 km distant from the epicentral area (Kämpf et al., 1989; Stejskal et al., 2008 and references therein). In the initial phase of the earthquake swarm, the discharge of the whole hydrogeological structure of the spa increased by about 30%, which lasted until 1988. However, the responses of the individual springs were considerably different. Precursory type changes were recognized

as an anomalous increase of water temperature of up to 3 °C at some springs in the period from several months to one month before the beginning of the earthquake swarm. Groundwater levels in four hydrological wells at epicentral distances from 0 to 30 km were analyzed by Gaždová et al. (2011) for the period 2000–2010. A noticeable drop in water level in all wells was observed in the period of the  $M_L$  3.8 swarm in 2008. However, a possible link origin of this anomaly to the hydrologic regime of the area was not examined.

Monitoring of mineral spring water in Wetztinger/Bad Brambach by Heinicke and Koch (2000) in the period of 1989–1999 revealed a number of anomalies in overflow of spring water lasting for few days, which were associated with the occurrence of a single local earthquake. Monitoring of the Bad Brambach springs during the 2000 swarm and extending the monitoring to the Cheb Basin confirmed possible precursory character of the anomalies in Bad Brambach (10 km W from the epicenter (Koch et al., 2003)). The aquifer system in Bad Brambach also reacted due to the 2008 swarm (Koch and Heinicke, 2011). However, continuous soil gas monitoring of carbon dioxide and radon at two sites in the NK focal zone did not find any variations of  $CO_2$  concentration during the 2008 earthquake swarm (Faber et al., 2009).



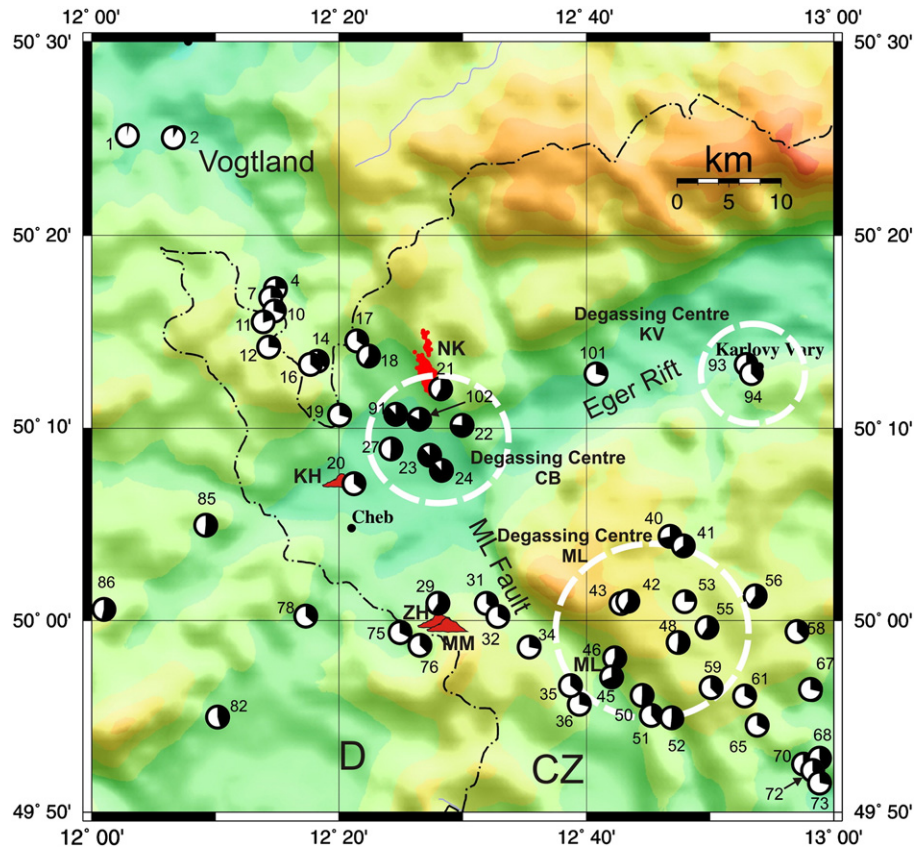


**Fig. 14.** Topographic map of West-Bohemia/Vogtland with the distribution of degassing locations (small numbers identify the degassing locations after Geissler et al., 2005). The black quarters of the circles correspond to the portions of mantle-derived helium related to the subcontinental mantle reservoir ( $^3\text{He}/^4\text{He} \approx 6.5\text{Ra}$ ; Gautheron et al., 2005). The data stem from Weinlich et al. (1999), Geissler et al. (2005) and Bräuer et al. (2011) (NK = Nový Kostel focal zone; CB = Cheb Basin; ML = Mariánské Lázně; KV = Karlovy Vary). Red points indicate the epicenters within NK and red triangles the volcanoes (KH = Komorní Hůrka; ZH = Železná Hůrka; MM = Mýtina Maar).

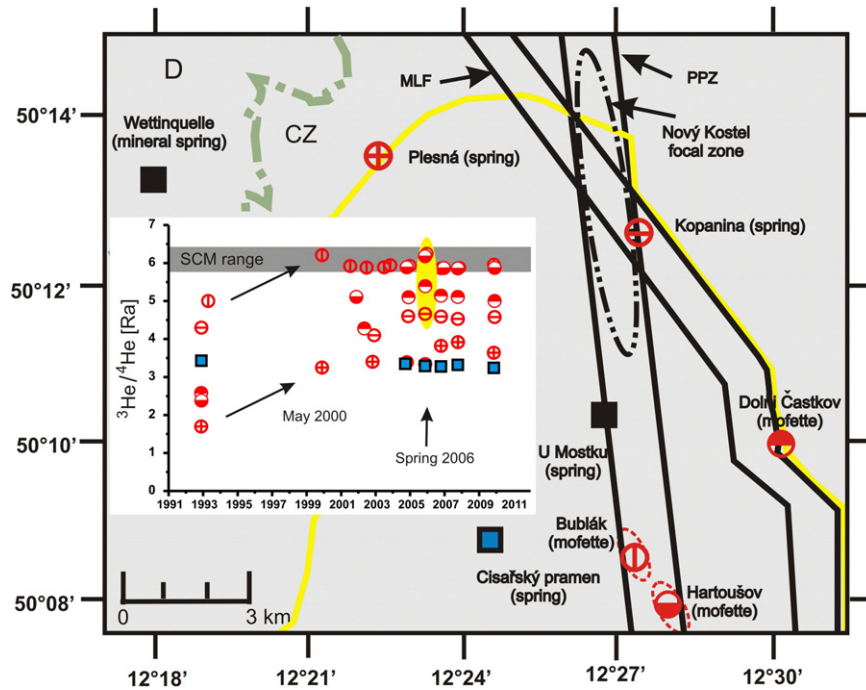


**Fig. 15.** Monitored locations in relation to the major faults and to the Nový Kostel focal zone (yellow = border of the Cheb Basin; MLF = Mariánské Lázně fault zone; PPZ = Počátky-Plesná fault zone; the dotted ellipses at Bublák and Hartoušov indicate the mofette fields). The inset shows variations of the  $^3\text{He}/^4\text{He}$  ratios from repeatedly sampled degassing locations in the Cheb Basin between 1993 and 2010. SCM (the  $^3\text{He}/^4\text{He}$  subcontinental mantle range) was taken from Gautheron et al. (2005). The yellow ellipse points to the increase of  $^3\text{He}/^4\text{He}$  ratios at sampled locations along the PPZ and MLF in spring 2006. The symbols in the inset and in the map are the same; circles mark locations with increased  $^3\text{He}/^4\text{He}$  ratios since 1993. The blue squares correspond to a gas-rich location with nearly constant  $^3\text{He}/^4\text{He}$  ratios. The helium data stem from Bräuer et al. (2009) supplemented by the latest unpublished data.

#### 6.4. Summary

CO<sub>2</sub> in mineral spring and mofettes in West Bohemia/Vogtland stem from the upper mantle; according to isotope studies, the three degassing centers are probably supplied by magmatic fluids from separated magma reservoirs at the Moho depths. In the Cheb Basin, the portion of mantle-derived helium was the highest at the PPZ where the subcontinental helium isotope signature indicates fluid transport pathways down to the deep lithospheric mantle. The observed temporal increase of the helium isotope ratios ( $>6$  Ra) before the 2000 and 2008 earthquake swarms might point to the occurrence of magma movements beneath the CB. The co-seismic change of isotope signatures of CO<sub>2</sub> and helium might be related to a release of crustal-derived volatiles due to fracturing and their admixture to the steadily ascending mantle-derived flow. The observed pre-seismic decrease of  $^3\text{He}/^4\text{He}$  ratios, simultaneous increase of the CO<sub>2</sub> emission rate and groundwater level changes probably origin in strain changes of the rock associated with the preparatory phase of earthquake swarms. Significant hydrologic anomalies were found during the M<sub>L</sub> 4.6 swarm of 1985/86 and M<sub>L</sub> 3+ swarms in 2000 and 2008.

#### 7. Earthquake swarm triggering

In this chapter we give a review of seismological studies aimed to identify the forces that are responsible for triggering and driving activity of the West Bohemia/Vogtland swarms. The principal question relates to the existence of external forcing that would bring the fault zone to the failure and possibly also keep the activity running. The primary focus is kept on fluids – mainly pressurized CO<sub>2</sub> and water. For this purpose the methods of statistical seismology, Coulomb stress analysis, and fluid pressure propagation were used (for details, see Horálek and Fischer, 2008).

Statistical parameters of magnitude and time occurrence of events differentiate earthquake swarms from mainshock–aftershock sequences. The absence of a mainshock and dominance of small events in swarms implies high *b*-values of their Gutenberg–Richter distribution, which typically exceed 1 and can reach up to 2.5 compared to *b*-values  $\leq 1$  for mainshock–aftershock sequences. However, this holds probably for volcanic swarms only, because the *b*-values of intracontinental swarms are only about 0.8 (Ibs-von Seht et al., 2008). In terms of their occurrence in time, the rate of aftershocks *N* typically decays with time measured from mainshock according to the Omori law  $N(t) = (c + t)^{-p}$ , where *t* is the time after the mainshock and *c* and *p* are fault-dependent constants. Omori law is also related to a power-law decay of interevent times measured between consecutive events. Following Molchan (2005), the interevent time distribution of the random occurrence of background seismicity decays exponentially, while the correlated seismicity is expected to obey the Omori law. This corresponds to the power-law decay of interevent time distribution. Thus the interevent time distribution is generally bimodal in earthquake sequences: a superposition of a power-law component from triggered aftershocks due to stress transfer at short time intervals and an exponential component at longer intervals from spontaneous events (Touati et al., 2011). The Omori-decay and the character of interevent time distribution for earthquake swarms is subject of research and will be addressed below for the case of West Bohemia/Vogtland.

##### 7.1. Correlation of seismicity in the whole West-Bohemia/Vogtland

Detailed analysis of space-time distribution of hypocenters in West Bohemia/Vogtland (Fig. 6) shows that the seismic activity can alternate among focal zones as well as it can occur simultaneously in different focal zones. Horálek and Fischer (2008, 2010) analyzed the time and space separation of consecutive events in the dataset of the whole West Bohemia/Vogtland region and found that the frequency of the

distances between consecutive events showed two maxima (see Fig. 9 in Horálek and Fischer, 2008) separated by a distance of 5 km. The first maximum at small distances corresponds to the event pairs occurring during individual swarms (clustered events), whereas the second maximum at larger distances is related to switching of the activity between distant focal zones. To quantify possible correlation of distant activity, Horálek and Fischer (2010) separated the seismic dataset from the period between 1991 and 2009 into two subsets: (1) all event pairs and (2) distant event pairs, which were separated by a distance larger than 5 km and analyzed their interevent time distribution. The probability density function (Fig. 7b) of interevent times for all consecutive event pairs and distant event pairs shows a bimodal distribution with a power-law dependence at short interevent times and exponential decay for larger interevent times. The power-law distribution is not surprising for all event pairs, because of the large influence of nearby events from individual swarms that are undoubtedly correlated. However, the power-law distribution for distant event pairs suggests that the small and distant events are correlated, as well. This is verified by creating a random catalog of the same size and with events whose origin times occur randomly within the period of observation. The probability density of this random event occurrence corresponds to the Poisson distribution, which significantly deviates from the probability density function observed for distant event pairs. In particular, it was found that the distant event pairs separated by intervals smaller than 40,000 s (about 11 h) showed an increased occurrence compared to the case of their random occurrence. Accordingly, Horálek and Fischer (2010) inferred that this could be attributed to triggering force acting in the broader area of West Bohemia/Vogtland.

##### 7.2. Swarm triggering as a result of elastic stress transfer

The magnitude and interevent-time distributions of earthquake swarms in West Bohemia/Vogtland were analyzed in order to find different characteristics from mainshock–aftershock sequences. Neunhöfer and Hemmann (2005) estimated *b*-values for 73 swarms in the whole region in the time span between 1903 and 1999. They found that while the *b*-values considerably varied between about 0.5 and 1.5, the intensive swarms in 1908, 1962, 1985/86, and 1997 showed a *b*-value of  $\sim 1.0$ . Similarly, a *b*-value of about 1.0 was estimated for the complete swarm of 2000 (Hainzl and Ogata, 2005; Tittel and Wendt, 2003). Hainzl and Fischer (2002) investigated the *b*-value for the individual phases of the 2000-swarm and found a decrease from about 1.3 in the first swarm phase down to 0.8 in the fourth and the following phases that was accompanied by the increase of the mean seismic moment. A sudden *b*-value decrease from 1.1 to 0.9 was also observed in the 1997 swarm (Cíž and Rudajev, 2001).

Hainzl and Fischer (2002) investigated also the interevent-time distribution of the 2000 swarm and found that it obeys a power-law  $T^{-1.5}$  except for the first swarm phase, which showed an exponential distribution indicating non-correlated swarm events. Thus, they inferred that the 2000 swarm was triggered by an increase of the fluid-pore pressure and further driven by self-organization due to a local stress transfer. Similar results were obtained by Hainzl and Ogata (2005), who applied the stochastic ETAS (epidemic-type aftershock sequence) analysis to the 2000 swarm. This model extends the Omori law and assumes that each event has a magnitude-dependent ability to trigger its own aftershocks, i.e. to drive the seismicity. The inversion of the seismic data provided the rate of internal and external triggering which Hainzl and Ogata (2005) attributed to the effect of the stress transfer and of the fluid signal, respectively. They found that the stress transfer induced most of the swarm events while the external force associated with the fluid pressure triggered only a few percent (about 5%) of them, mainly at the beginning of the activity and after periods of quiescence (Fig. 16a).

The Omori-like character of the 2000 swarm was analyzed by Hainzl and Fischer (2002) who identified 80 mainshocks within the 2000

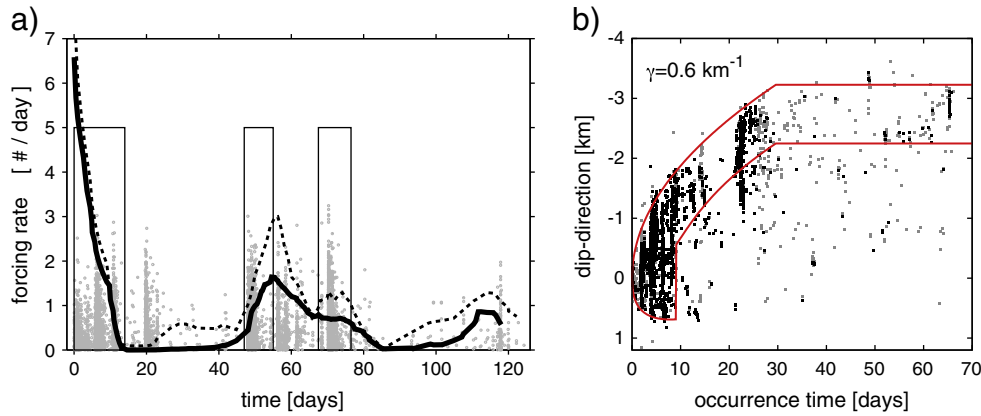


**Fig. 16.** (a) ETAS analysis of the 2000 swarm; external forcing (solid curve) obtained by the ETAS model needed to trigger and drive the activity of the 2000 swarm that is shown by a magnitude–time plot (gray dots), phases in which the spatial spreading of the swarm activity indicates pore pressure diffusion are indicated by boxes; adapted from Hainzl and Ogata (2005). (b) Application of the hydrofracture model to the migration pattern of the 2008 swarm in dip-direction. The fit yields a normalized gradient of  $\gamma = 0.6 \text{ km}^{-1}$ . The backfront position as well the maximum up-dip extension of the seismicity cloud are direct forecasts of the model. Black dots mark  $M \geq 0.5$  earthquakes whereas gray dots refer to smaller events; according to Hainzl et al. (2012).

swarm and stacked the corresponding aftershock series, which resulted in a characteristic Omori-law decay with  $p \sim 1.0$ . Similarly, Fischer (2003) found  $p$ -values in the range from 0.5 to 1.9 for the individual phases of the 2000 swarm. This indicates that the West Bohemia earthquake swarms can be viewed as a set of overlapping mainshock–aftershock sequences in time and space and conforms the understanding of earthquake swarms as a result of heterogeneous stress and strength field to a missing well-developed fault plane (Mogi, 1963). The fact that the Omori-like decay is easily observable in the West Bohemia/Vogtland swarms indicates that these swarms probably represent end member of the family of the earthquake swarms that spans from purely externally driven swarms in volcanic environments to the tectonic-like West Bohemia/Vogtland swarms. Kárník and Schenková (1987) noted that the 1985/86 swarm differed from a typical swarm-type activity in its time pattern, which resembled a single disintegrated mainshock preceded by foreshocks and followed by aftershocks.

Triggering mechanisms acting in the 2000 swarm were investigated by Fischer and Horálek (2005) on the basis of space–time relations between consecutive  $M_L > 0.5$  earthquakes. The spatial and temporal distributions of all event pairs (Fig. 17a) and fast event pairs (Fig. 17c) with interevent velocities larger than  $100 \text{ m s}^{-1}$  show a distinct prevalence of the immediate aftershocks occurrence along the direction of  $30^\circ$  to  $40^\circ$  from horizontal, which corresponds to the prevailing slip-parallel

direction of source mechanisms. While the polar plot of all the event pairs displays nearly oval form, the fast event pairs show a lobe-like character with minimum occurrence in the slip-perpendicular direction, which resembles the static and dynamic Coulomb stress change, respectively (Fig. 17b). This suggests that the static stress changes were significant in triggering subsequent aftershocks close to prior earthquakes, while a triggering effect due to dynamic stress changes took place mainly at larger distances and smaller time scales. The small amplitudes of the stress changes, which are just fractions of the earthquake stress drop, could be accountable for triggering only in case of critical loading of the fault plane. This is precisely the case when pressurized fluids, which increase the pore pressure and reduce the friction, bring the fault to the limit of stability.

### 7.3. Migration of hypocenters and fluid and magma triggering

Migration of foci, a typical feature of earthquake swarms, was first reported by Antonini (1988) who interpreted a systematic south-to-north trending migration in the swarm of 1985/86 by a successive release of tectonic stress accumulated along the MLF. A clear foci migration was observed for the ensuing swarms in 1997, 2000, 2008, and 2011 thanks to the precise relocations discussed above. The 2000 and 2008 swarms show a self-similar well-developed trend (Fig. 9): the first events of both swarms occurred at the bottom of the fault segment

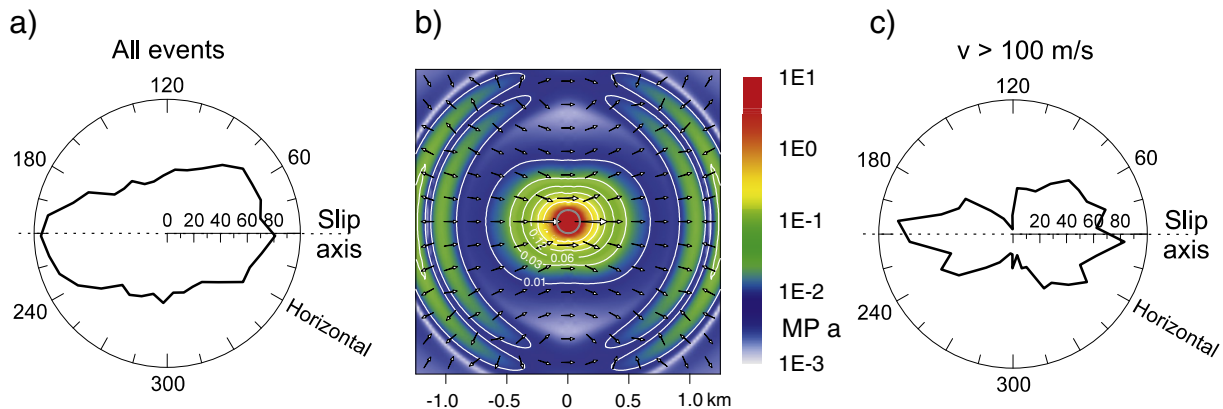


**Fig. 17.** Angular dependence of the rate of immediate aftershocks evaluated using a step of  $10^\circ$ ; all aftershocks in panel (a); aftershocks linked by speed higher than  $100 \text{ m/s}$  in panel (c). The slip axis is derived using the most common source mechanism showing rake angle of  $30^\circ$ – $40^\circ$ . Space–time distribution of the complete stress field (dynamic and static) in panel (b) resolved on the fault plane surrounding the rupture induced by an instantaneous stress drop of  $10 \text{ MPa}$  due to strike slip on a circular area with radius of  $100 \text{ m}$  in a homogeneous half-space. Only the shear stress vector (traction) is given because the normal stress is zero. The stress field breaks with time into the permanent (static) part as a result of the near-field deformation and the transient (dynamic) part carried by the propagation of seismic waves. Adapted from Fischer and Horálek (2005).



and the final events in the uppermost tail. Nevertheless, a more detailed space-time distribution of the foci shows a fairly different pattern: the counter-clockwise migration of the 2000 swarm and a gradual upward migration of the 2008 swarm. The hypocenter migration of the 2011 swarm was rather different: the activity started at 8 km depth at the top-northern edge of the 2008-swarm segment and migrated step-wise to the north and slightly downwards with high density of hypocenters. After a two-day gap a fast vertical migration with smaller event density took place for the next three days between the depths of 9 and 7 km.

The migration of hypocenters suggested relevance of pressurized fluids in the swarm triggering (Špičák and Horálek, 2000). Later it was pointed out that the conspicuous migration of the 2000-swarm activity starting at the bottom part could be explained by diffusion of pressurized fluids injected into the permeable fracture zone (Parotidis et al., 2003). This approach is based on the assumption that the earthquakes map the advance of the pore pressure front; this means that the seismic rupture does not advance or fall behind the pore pressure front. Provided that the hydraulic diffusivity of the rock is constant and the pore pressure field is decoupled from seismic rupturing and related stress changes, the disturbance of the pore-pressure field can be described by the diffusion equation. A solution of this equation in homogeneous isotropic medium results in a distance  $r$  representing the propagating pore pressure front by  $r = \sqrt{4\pi Dt}$ , where  $t$  is the time from the start of injection (Shapiro et al., 1997). By fitting a parabolic envelope to the  $r(t)$  plot of the migration of the foci, Parotidis et al. (2003) obtained a diffusivity of  $0.27 \text{ m}^2 \text{ s}^{-1}$  for the 2000 swarm. Similar diffusivity was observed by Hainzl and Ogata (2005) who fitted the parabola only to the externally triggered events obtained by declustering the catalog.

However, rocks are anisotropic because of strong heterogeneities like faults acting as permeable channels on one hand, or as impermeable barriers on the other hand. Besides, stress gradients due to density contrasts between fluids and rock or heterogeneous tectonic stress occur. The combination of both effects results in a preferred orientation of the fluid flow and seismicity spreading. This was pointed out by Hainzl et al. (2012) who found that the migration of the 2008 swarm hypocenters requires three times higher hydraulic diffusivity for up-dip direction than for the down-dip direction. To account for the asymmetry they applied hydrofracture model of Fischer et al. (2009) and Dahm et al. (2010) that allows for asymmetric growth of the seismicity accompanying the hydraulic fracture due to the stress gradients. Application of the hydrofracture model presumes that fluid pressure exceeds the minimum confining pressure, which results in co-seismic tensile fracture opening. It would however work also in the case of a smaller fluid pressure, because the Coulomb failure criterion is easier fulfilled in the up-dip direction of hydraulic gradient. The model provided excellent fit to the observed spreading of hypocenters (Fig. 16b) with the resulting gradient of  $0.6 \text{ km}^{-1}$  that corresponds to the injection overpressure of about 20 MPa for water as the injected fluid.

A possible role of magma intrusion in swarm triggering was examined, as well. According to Šafanda and Čermák (2000), the subsurface heating caused by magma intrusion at the assumed focal depth (horizontally infinite 50 m thick sill with temperature of  $1100^\circ \text{C}$ ) is not detectable by direct geothermal measurements due to the long delay of the heat pulse (100 ka) and only 2% increase of heat flux. However, a slightly faster response of the surface temperature would occur (Kohl et al., 1998) if convective heat transfer due to  $\text{CO}_2$  flow was considered. Dahm et al. (2008) proposed an interpretation of the migration of the 2000-swarm hypocenters by a magma intrusion. The analysis of the theoretical 3D shape of intrusions constrained parameters of the fluid, the surrounding rock and stress showing that the 2000 swarm could have been driven by a fluid intrusion. The possible fluid intrusion would be of a similar density to the density of the rock (magma), and inclined to the maximal principal stress, which would cause shear displacement additional to opening.

Possible role of fluids might be also indicated by an anomalous  $v_p/v_s$  ratio found in the source volume of earthquake swarms in the NK focal zone. In general, the rocks in the crust display quite stable  $v_p/v_s$  of about 1.7 and any deviation from this value points to the possible presence of fluids. Vavryčuk (2011b) analyzed moment tensors of tensile earthquakes that occurred during the 1997 and 2008 swarms and determined the  $v_p/v_s$  ratio from the slope of the linear relation between the ISO and CLVD moment tensor components. Both swarms showed anomalous small  $v_p/v_s$  in the focal volume, 1.45 for the 1997 swarm and 1.35 for the 2008 swarm. Dahm and Fischer (2013) used the double-difference version of the Wadati method to determine  $v_p/v_s$  during the 1997, 2000, and 2008 swarms. For all swarms a strong temporal decrease of  $v_p/v_s$  before and during the main activity of the swarm down to 1.3 was resolved with a recovery of  $v_p/v_s$  to background levels at the end of the swarms. The extremely small velocity ratios are interpreted in terms of the Biot–Gassmann equations, assuming degassing of over-saturated fluids during the beginning phase of the swarm activity.

#### 7.4. Other models of the swarms

Hainzl (2004) proposed a model of the 2000 swarm consisting of a planar brittle patch placed in a 3-D elastic half-space with geometry similar to the 2000-swarm that includes two triggering mechanisms: fluid injection and stress changes. The tectonic stress keeps the patch subcritically loaded until the pore pressure of diffused fluids from the underlying fluid source brings it to failure, which is governed by the Coulomb failure criterion. Then, the earthquake activity is governed by the stress changes due to the co-seismic and post-seismic slip, which accounts for a drop of friction due to a slip from its static to its dynamic value and its subsequent recovery so that mutual triggering between ruptured cells occurs. The combination of both mechanisms succeeded to reproduce, among others, the event magnitudes, the  $b$ -values, and the Omori-type clustering of the earthquakes in time, and the diffusion-like spreading of hypocenters below a parabolic envelope in the  $r(t)$  plot. While the fluid diffusion is only reflected in the spatio-temporal migration, the stress triggering is responsible for all the other characteristics.

The overlapping activity of the 2000 and 2008 swarms has opened the question of the underlying mechanisms that led to the reactivation of the same fault plane after only 8 years (see Fig. 8 and 9). This was addressed by Hainzl et al. (2012) who showed that the 2008 swarm can be understood partially as a simple rupture extension of the pre-existing rupture area of the 2000 swarm (Fig. 18a). To examine the reason for repeated rupturing of the fault plane they calculated the Coulomb stress changes induced by precursory events of the 2000 and 2008 swarms at the location of each swarm earthquake. They found that about 60% of events occurred in regions unloaded by the preceding activity with stress deficit up to 20–30 MPa (Fig. 18b). Thus, external loading must be considered when bringing the fault patch to the failure. Assuming that observed stress deficits had to be compensated by fluid injection, an underlying pore-pressure increase in the range of 20–45 MPa was necessary.

Most of the reviewed studies interpret the role of fluids in terms of the effect of their high pressure that destabilizes the fractures. This results in their partial opening and associated shearing. Heinicke et al. (2009) proposed different physical mechanisms consisting of hydrothermal alteration of the minerals by the circulating aqueous  $\text{CO}_2$ -saturated fluids at optimal P–T conditions present in the seismogenic depths. According to this study, the walls of fractures are being dissolved in contact with a steady-state flow of the acid fluid phase, and the stressed fault zone is gradually weakened, which would result in its repeated fracturing. Associated compaction of fractures would be accompanied by moment tensors of compressional type. Interestingly, such source mechanisms often occur at the beginning of the swarms as was the case of the 1997 swarm (Horálek et al., 2002) and the 2008

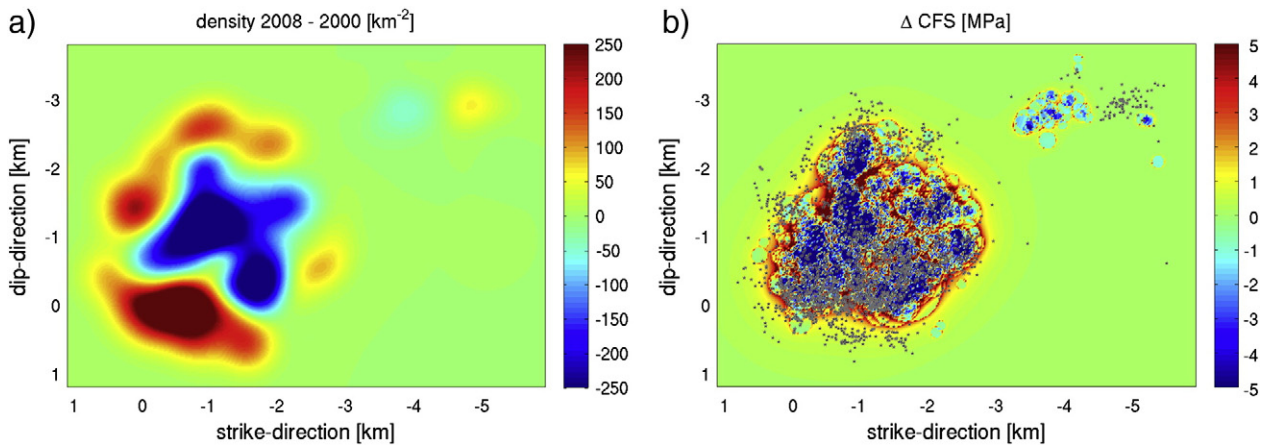


**Fig. 18.** Coulomb stress analysis of 2000 and 2008 swarms. (a): Difference of the  $M_L \geq 0.5$  event densities in the swarms 2008 and 2000. Positive values indicate areas with significantly more activity during the year 2008 than 2000 whereas negative values mark active areas in 2000, which were significantly less active in 2000. (b): Cumulative stress changes related to the year 2000 swarm activity in comparison with the locations (points) of the swarm earthquakes in the year 2008. The assumed earthquake stress drop used to estimate the rupture areas is 1 MPa.

swarm (Vavříčuk, 2011b). We however infer that the ambiguity of non-DC components of the moment tensors obtained by different authors mentioned in Section 5.4 does not allow us to draw conclusions as regards to the possible role of fluids in seismic fracturing. To complete the review of possible triggering mechanisms, the possible effect of the Earth's tides should be noted. This was analyzed by Fischer et al. (2006) who showed that increased occurrence of the earthquake swarms in the period of 1991–2005 near the fortnightly maximum of tidal extensive normal stress was not statistically significant, and this led to rejection of tidal triggering hypothesis.

### 7.5. Summary

The occurrence of swarm earthquakes in the whole West-Bohemia/Vogtland is found correlated at interevent times below 11 h, which points to a common triggering force. The activity of swarms on the scale of NK zone appears to be driven by stress transfer among individual earthquakes. This is indicated by Omori-type decay, ETAS analysis, and the Coulomb stress analysis of the 2000 and 2008 swarms. However, the latter two methods revealed repeated external forcing (possible fluid injection) during these swarms, which is probably also responsible for the initial triggering of the activity. In addition, pressurized fluids are presumed to keep the near-critical loading of the focal zone that decreases the effective normal stress and makes the stress triggering possible, despite the tiny stress changes due to the running activity. The role of the high fluid pressure is found from the hypocenter spreading, which is consistent with the pore pressure diffusion models and even better with the model of hydraulic fracture with preferential growth in the up-dip direction. An independent indication of high fluid pressure comes from anomalously low  $v_p/v_s$  ratios found in the focal zone that points to gaseous fluid phase. A different concept of swarm triggering presumes that the fault zone is destabilized by hydrothermal alteration of minerals; the resulting collapse of the newly created pore space is however not clearly supported by source moment tensors.

## 8. Discussion and conclusions

### 8.1. Summary of the existing results

The presented review of the geodynamic processes in West Bohemia/Vogtland can be summarized as follows.

- (1) The present seismic activity is concentrated at the intersection of the Eger Rift and the Regensburg–Leipzig–Rostock Zone where the Tertiary Cheb Basin was formed due to the subsidence along the

Mariánské Lázně Fault. While in the northern part of the region the solitary events prevail, the earthquake swarms are typical for the broader area of the Cheb Basin. The area close to Nový Kostel stands out with more than 80% of seismic moment released during the past 20 years. The maximum hypocenter depths vary from 10 to 25 km with an increasing trend towards NW; the deepest hypocenters in the NK zone occur at 12 km.

- (2) Seismic methods show laminated lower crust with the top at about 27–28 km in the area of earthquake swarms, which could correspond to alternating rock types or melt. However, no direct evidence for the existence of a plume in the lower crust or the upper mantle was supplied.

- (3) The area is typified by intense  $\text{CO}_2$  degassing and Quaternary volcanism. The dating of the onset of  $\text{CO}_2$  escapes coincides with the age determinations of eruptions of three documented volcanoes in about 0.78 to 0.12 Ma. Isotope ratios of carbon and helium show magmatic origin of the escaping  $\text{CO}_2$ , which is one of the evidence for the magmatic activity in the lower crust/upper mantle. Similar depth of 25–40 km is provided by analysis of mantle xenoliths from 0.29 Ma old volcanics, which could correspond to the depth of origin of rising magma. This indicates that the  $\text{CO}_2$  escaping at present originates from a similar depth as the magma that erupted in the Quaternary volcanoes.

- (4) The deep origin of  $\text{CO}_2$  implies that the gas must pass, most probably along permeable fault zones, through the seismogenic depth to the surface, and thus can take place in the seismogenic processes. The possible role of fluids is indicated by analysis of triggering of swarms that occurred in the NK zone. It was found that the external forcing is needed to trigger the swarm activity and the elastic stress transfer does not always suffice to drive the running swarm. Intra-plate tectonic loading rates are found insufficient for stress recovery alone to trigger swarms with such short recurrence intervals as seen at NK in the past 25 years. On top of tectonic loading pressurized fluids seem to be another candidate for external forcing that would be also consistent with the spreading of activity observed in hypocenter locations. The role of fluids is twofold: besides external forcing, the acidic pressurized fluids could weaken the fault zone — both mechanically by decreasing the friction, and chemically by hydrothermal alteration of the minerals.

- (5) In contrast to some previous studies presenting the fault zone of Nový Kostel as a simple steeply dipping fault plane, the precise earthquake locations, focal mechanism determinations and namely the hypocenter distribution of the recent 2011 swarm show that the fault zone is rather complex, composed of several intersecting segments. This also holds for the majority of earthquakes of the

2008 swarm, which occur on two principal conjugate faults oriented optimally for shearing with respect to the tectonic stress in the region.

The fact that the present epicenter distribution in the region overlaps roughly with the occurrence of gas escapes (Fig. 20) could support possible relation between CO<sub>2</sub> flow and earthquake swarm activity. There are only few exceptions from this correlation: earthquake epicenters in Vogtland (focal zone 6 – Schöneck) with missing CO<sub>2</sub> degassing and the absence of seismic activity in few CO<sub>2</sub> escape areas in the south. However, the present earthquake swarm distribution that dominates in the area of Nový Kostel since 1985 may represent only a short episode in a larger-scale migration of the earthquake swarms. According to Fischer et al. (2010), the repeated swarm activity in the Nový Kostel zone within the past period would require an unrealistic loading rate of about 1 cm/year if the released slip would be equal to the cumulative loading. The high loading rate would not be necessary if the swarm recurrence interval would be evaluated for the whole region of West Bohemia/Vogtland and the activity in the period from 1872 to 1908 would be considered.

## 8.2. A broader view of the geodynamics in time and space

To extend the time and space view of the activity we checked the available information about the macroseismically documented seismic activity in the 19th century and disclosed that the 1824 swarm occurred at different location compared to the present activity and the swarms at the turn of the 19th and 20th centuries. The area of maximum intensities of the 1824 swarm (Fig. 19) in the isoseismal map of Knett (1899) shows clearly different position than the epicentral areas of the 1897 swarm reported by Credner (1898) and of the 1903 and 1908 swarms estimated by Procházková (1987). This is further underlined by Knett (1899) who argues that the 1824 swarm was located close to Hartenberg in contrast to the 1897 swarm, which occurred near Kraslice. However, no adequate data about swarm

activity prior to 1824 was found, which was already mentioned by Kárník (1963) who also brought preliminary analysis of the M<sub>L</sub> 2.7 swarm in 1962. Kárník (1963) has located the 1962 swarm to the Kraslice region and noted that the activity since 1897 has been switching between the areas of Kraslice and Bad Brambach, which he termed as a “twin-focus” activity.

According to available data on historic seismicity, few notable facts turn out (Fig. 19): (i) the earthquake swarm occurrence has shown pronounced migration within the area of 15 × 15 km during the past 200 years; (ii) the 1824 swarm occurred in the area of Hartenberg–Oloví, which has displayed no earthquake activity within the past 22 years of continuous monitoring (see Fig. 6); (iii) the area of 1824 swarm is free of any present CO<sub>2</sub> escapes and no mineral springs are documented there in the past (T. Vylita, personal communication). The absence of present seismicity in the location of 1824 swarm represents a unique evidence of a long-term migration of the earthquake swarm activity. In particular, the data on the changing position of epicenters of the 1824–2011 swarms indicate that the leading role in the whole area is transferred among different focal zones and that the major focal zone may become even quiet, which is probably the case of Hartenberg–Oloví. In this context it should be noted that while in the Kraslice–Bad Brambach area quite dense distribution of microearthquake swarms occurs (Fig. 6), there is a clear gap of epicenter occurrence east of MLF where the 1824 swarm occurred. Hence, it seems that according to the activity, the major focal zone migrates in a following way. About 1824: Hartenberg–Oloví; 1897–1962: Kraslice–Bad Brambach; and 1985–2011: Nový Kostel (Fig. 19).

The migration of swarms invokes a question about the stability of gas escape areas. As documented by travertine dating, CO<sub>2</sub> degassing in Karlovy Vary started about 0.23 Ma, which probably dates the onset of the mantle CO<sub>2</sub> flow in the whole West Bohemia/Vogtland region. However, in contrast to the earthquake swarms, no significant fluctuations of CO<sub>2</sub> emanations were observed within past 200 years, which indicates that the occurrence of CO<sub>2</sub> flow is more stationary than the earthquake swarm occurrence.

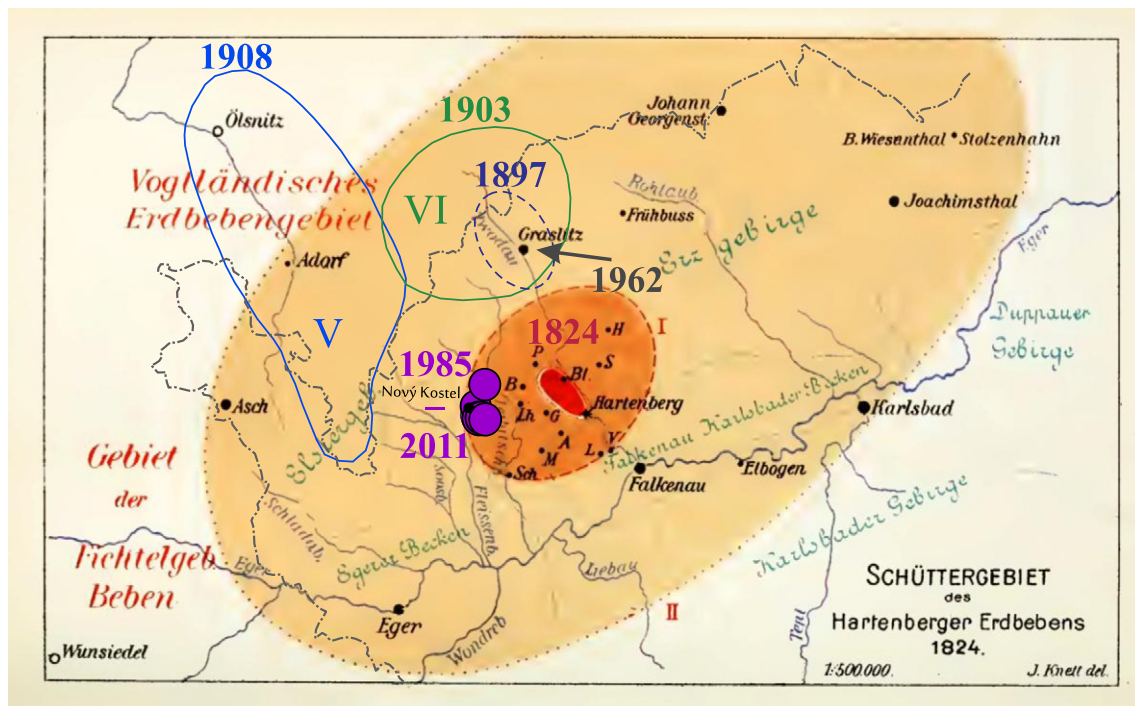


**Fig. 19.** Isoseismal map of the 1824 earthquake swarm near Hartenberg (Knett, 1899) supplemented by the occurrence of later swarms. The isoseists of the 1824 swarm indicate strong (I) and felt (II) shaking, the meaning of selected abbreviations is: Bl = Bleistadt (Oloví), B – Bernau, P – Prünles (Studenec), G – Gossegrün (Krajčová), L – Lauterbach (Čistá). Dashed dark blue line encompasses the area where the 1897 swarm commenced (Credner, 1898), the isoseists of the 1903 and 1908 swarms are adapted from Procházková (1987). The gray arrow indicates position of the swarm 1962 (Kárník, 1963). The violet circles show the epicenters of M<sub>L</sub> 3+ earthquakes of 1985–2011 swarms in the Nový Kostel zone.



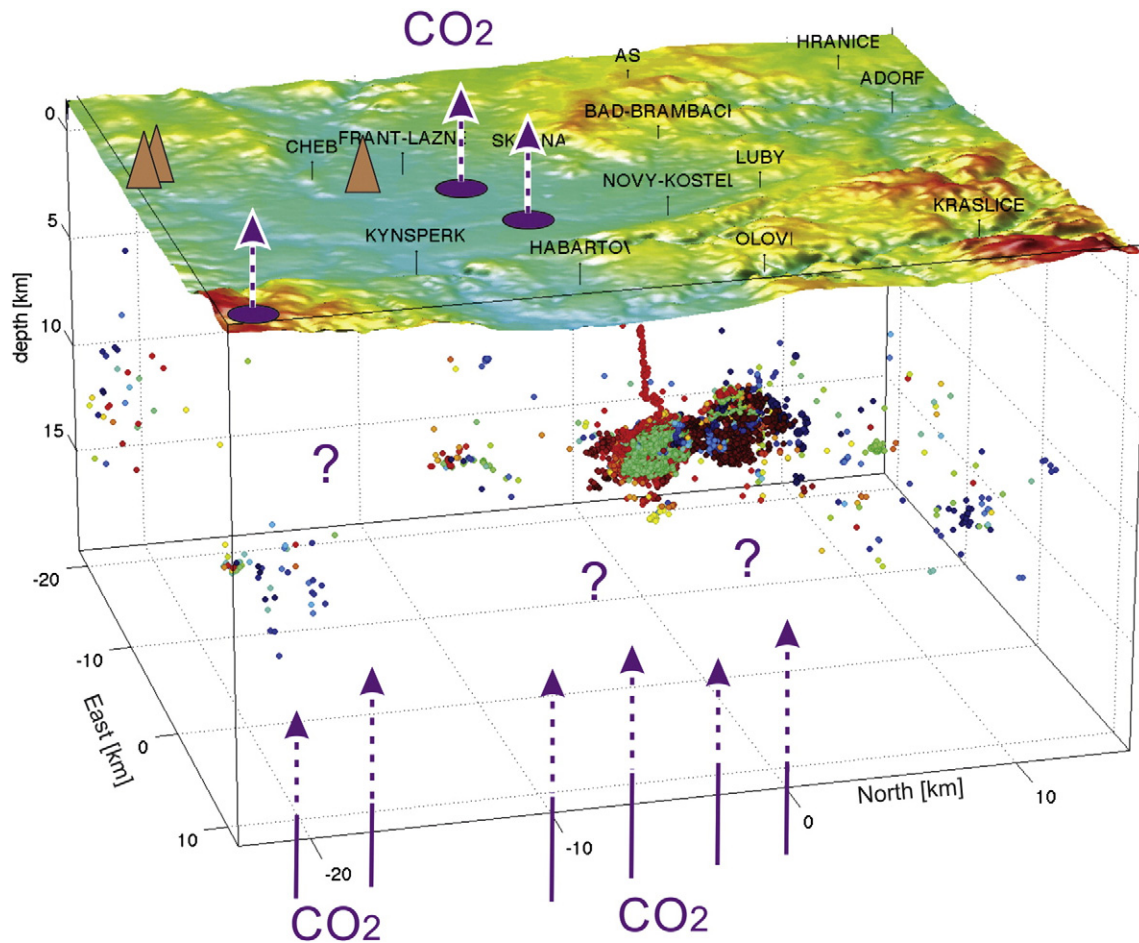


**Fig. 20.** Schematic cartoon illustrating the state-of-art knowledge about the principal geodynamic processes in West Bohemia/Vogtland. The hypocenters are indicated by filled circles using time color scale from Fig. 7. Three main degassing centers are (Prameny, Soos, Bublák – blue ellipses) and three Quaternary volcanoes (KH, ZH, and MM – brown triangles) are indicated. Topography is indicated as colored map and ranges between 400 and 800 m.

The migration of the major focal zone among gas-escape and gas-free areas indicates that it might be difficult to find a direct link between the earthquake swarm occurrence and the gas flow. The earthquake swarm occurrence is consistent with the models of earthquake triggering by fluids and some correlation, though not always straightforward, between the swarm occurrence and anomalies in fluid emanations is documented. Thus, we can say that the earthquake swarms and magmatic  $\text{CO}_2$  degassing are manifestations of the geodynamic activity of the area; they are linked together, though fluids are probably not the only triggering factors of the swarms. Besides, our data on the scale of present occurrence of the earthquake swarms and  $\text{CO}_2$  escapes allow only for short-term correlation analysis, which is not sufficient for drawing conclusions of general validity. As an example, present concentration of the earthquake swarms in the area of Nový Kostel, which lies apart from the moffetes Soos and Bublák and from mineral springs in Bad Brambach could give impression of exclusive occurrence of earthquakes and  $\text{CO}_2$  escapes. However, only 100 years ago the earthquake swarms were concentrated close to Bad Brambach, where mineral springs do exist for much longer period.

### 8.3. Concluding remarks and prospects for further research

It should be noted that migration of seismicity on the scale of 100 years implies that the earthquake swarms in Nový Kostel may cease soon and another place in the area might overtake the leading role. This could be a guide for planning further research projects in order to employ the present period of strong activity that provides

high-quality seismological and other geoscience data on the ongoing geodynamic processes.

The existing results indicate that migration of pressurized fluids of mantle origin in the crust is involved in the earthquake swarm occurrence and triggering in West Bohemia/Vogtland. However, the particular mechanism of the interaction of the fluids, stress field, and fault fabric in generating the earthquake swarms is not fully understood. In order to get answers to these open questions, further interdisciplinary research is needed. This should target the possible existence of non-volcanic tremors that could bring an independent indication of pressurized fluid activity in the roots of faults, improving the detection capability of the seismic network to get a more detailed geometry of the fault zone, and also tomography studies including monitoring of the  $v_p/v_s$  ratios during swarms to get insight in the fluid flows and their possible phase changes. Beside continuing isotope geochemistry studies, a promising avenue is also precise source mechanism analysis that would allow for mapping pore pressure and stress changes during the swarm activity. This way the research of contemporary seismic activity and  $\text{CO}_2$  degassing in this natural laboratory could promote our understanding of the link among geodynamic processes in the area.

### Acknowledgments

We are grateful to Stephen Cox and one anonymous reviewer for their thorough reviews and valuable suggestions. The work of individual authors was supported by the Grant Agency of the Czech Republic under the grants No. P210/12/2451, P210/12/2336, 13-08971S, and P210/12/1491 and by the European Community's FP7 Consortium Project AIM



“Advanced Industrial Microseismic Monitoring”, Grant Agreement No. 230669 and by the Czech Ministry of Education research plan No. MSM0021620855.

## References

- Angelier, J., 2002. Inversion of earthquake focal mechanisms to obtain the seismotectonic stress IV – a new method free of choice among nodal lines. *Geophys. J. Int.* 150, 568–609.
- Antonini, M., 1988. Variations in the focal mechanisms during the 1985/86 Western Bohemian earthquake sequence – correlation with spatial distribution of foci and suggested geometry of faulting. In: Procházková, D. (Ed.), *Induced Seismicity and Associated Phenomena*. Geophys. Inst. Czechosl. Acad. Sci. Praha, pp. 250–270.
- Babuška, V., Plomerová, J., Fischer, T., 2007. Intraplate seismicity in the western Bohemian Massif (central Europe): a possible correlation with a paleoplate junction. *J. Geodyn.* 44, 149–159.
- Babuška, V., Plomerová, J., 2013. Boundaries of mantle-lithosphere domains in the Bohemian Massif as extinct exhumation channels for high-pressure rocks. *Gondwana Research* 23, 973–987. <http://dx.doi.org/10.1016/j.jgr.2012.07.005>.
- Bankwitz, P., Schneider, G., Kämpf, H., Bankwitz, E., 2003. Structural characteristics of epicentral areas in Central Europe: study case Cheb Basin (Czech Republic). *J. Geodyn.* 35, 5–32. [http://dx.doi.org/10.1016/S0264-3707\(02\)00051-0](http://dx.doi.org/10.1016/S0264-3707(02)00051-0).
- Behr, H.J., Dürbaum, H.J., Bankwitz, P., 1994. Crustal structure of the Saxothuringian Zone: results of the deep seismic profile MVE-90 (East). *Z. Geol. Wiss.* 22 (6), 647–769.
- Blecha, V., Štemprok, M., Fischer, T., 2009. Geological interpretation of gravity profiles through the Karlovy Vary granite massif (Czech Republic). *Stud. Geophys. Geod.* 53, 295–314.
- Bouchaala, F., Vavřík, V., Fischer, T., 2013. Accuracy of the master-event and double-difference locations: synthetic tests and application to seismicity in West Bohemia, Czech Republic. *J. Seismol.* 17, 841–859. <http://dx.doi.org/10.1007/s10950-013-9357-4>.
- Bräuer, K., Kämpf, H., Strauch, G., Weise, S.M., 2003. Isotopic evidence ( $^3\text{He}/^4\text{He}$ ,  $^{13}\text{C}/^{12}\text{C}$ ) of fluid-triggered intraplate seismicity. *J. Geophys. Res.* 108 (B2), 2070. <http://dx.doi.org/10.1029/2002JB002077>.
- Bräuer, K., Kämpf, H., Niedermann, S., Strauch, G., Weise, S.M., 2004. Evidence for a nitrogen flux directly derived from the European subcontinental mantle in the Western Eger Rift, central Europe. *Geochim. Cosmochim. Acta* 68, 4935–4937.
- Bräuer, K., Kämpf, H., Niedermann, S., Strauch, G., 2005. Evidence for ascending upper mantle-derived melt beneath the Cheb basin, central Europe. *Geophys. Res. Lett.* 32. <http://dx.doi.org/10.1029/2004GL022205> (L08303).
- Bräuer, K., Kämpf, H., Koch, U., Niedermann, S., Strauch, G., 2007. Seismically-induced changes of the fluid signature detected by a multi-isotope approach ( $\text{He}$ ,  $\text{CO}_2$ ,  $\text{CH}_4$ ,  $\text{N}_2$ ) at the “Wettnquelle”, Bad Brambach (Central Europe). *J. Geophys. Res.* 112. <http://dx.doi.org/10.1029/2006JB004404> (B04307).
- Bräuer, K., Kämpf, H., Niedermann, S., Strauch, G., Tesářík, J., 2008. Natural laboratory NW Bohemia: comprehensive fluid studies between 1992 and 2005 used to trace geodynamic processes. *Geochem. Geophys. Geosyst.* 9. <http://dx.doi.org/10.1029/2007GC001921> (Q04018).
- Bräuer, K., Kämpf, H., Strauch, G., 2009. Earthquake swarms in non-volcanic regions: what fluids have to say. *Geophys. Res. Lett.* 36. <http://dx.doi.org/10.1029/2009GL039615> (L17309).
- Bräuer, K., Kämpf, H., Strauch, G., 2011. Monthly monitoring of gas and isotope compositions in the free gas phase at degassing locations close to the Nový Kostel focal zone in the western Eger Rift, Czech Republic. *Chem. Geol.* 290, 163–176.
- Brückel, E., Bleibinhaus, F., Gosar, A., Grad, M., Guterch, M., Hrubcová, P., Keller, G.R., Majdański, M., Sumanovac, F., Tiira, T., Yliniemi, J., Hegedüs, E., Thybo, H., 2007. Crustal structure due to collisional and escape tectonics in the Eastern Alps region based on profiles Alp01 and Alp02 from the ALP 2002 seismic experiment. *J. Geophys. Res.* 112. <http://dx.doi.org/10.1029/2006JB004687> (B06308).
- Brudy, M., Zoback, M.D., Fuchs, K., Rummel, F., Baumgärtner, J., 1997. Estimation of the complete stress tensor to 8 km depth in the KTB scientific drill holes: implications for crustal strength. *J. Geophys. Res.* 102, 18453–18475.
- Chlupáčová, M., Skácelová, Z., Nehybka, V., 2003. P-wave anisotropy from the seismic area in Western Bohemia. *J. Geodyn.* 35, 45–57.
- Číž, R., Rudajev, V., 2001. Analysis of seismicity of Western Bohemian earthquake swarm areas. *Acta Montana* 121 (18), 5–13.
- Credner, H., 1876. Das vogtländisch-erzgebirgische Erdbeben vom 23. November 1875. *Z. Ges. Naturwiss.* 48, 246–269.
- Credner, H., 1898. Die sächsischen Erdbeben während der Jahre 1889 und 1897, insbesondere das sächsisch-böhmische Erdbeben vom 24. Oktober bis 29. November 1897. *Abhandlungen der mathematisch-physischen Classe der Königl. Sächsischen Gesellsch. d. Wissensch.* Band XXIV. No. IV, pp. 315–399.
- Dahm, T., Fischer, T., 2013. Velocity ratio variations in the source region of earthquake swarms obtained from arrival time double-differences. *Geophys. J. Int.* (accepted for publication).
- Dahm, T., Horálek, J., Šilený, J., 2000. Comparison of absolute and relative moment tensor solutions for the January 1997 West Bohemia earthquake swarm. *Stud. Geophys. Geod.* 44, 233–250.
- Dahm, T., Fischer, T., Hainzl, S., 2008. Mechanical intrusion models and their implications for the possibility of magma-driven swarms in NW Bohemia region. *Stud. Geophys. Geod.* 52, 529–548.
- Dahm, T., Hainzl, S., Fischer, T., 2010. Bidirectional and unidirectional fracture growth during hydrofracturing: role of driving stress gradients. *J. Geophys. Res.* 115 (B12), 322. <http://dx.doi.org/10.1029/2009JB006817>.
- DEKORP Research Group, 1988. Results of deep reflection seismic profiling in the Oberpfalz (Bavaria). *Geophys. J. Int.* 89, 353–360. <http://dx.doi.org/10.1111/j.1365-464X.1987.tb04430.x>.
- DEKORP Research Group, 1994. The deep reflection seismic profiles DEKORP 3/MVE-90. *Z. Geol. Wiss.* 22 (6), 623–824.
- Dreger, D.S., Tkalcic, H., Jonston, M., 2000. Dilational processes accompanying earthquakes in the Long Valley Caldera. *Science* 288, 122–125.
- Eckhardt, C., Rabbel, W., 2011. P-receiver functions of anisotropic continental crust: a hierarchical catalogue of crustal models and azimuthal waveform patterns. *Geophys. J. Int.* 187, 439–479.
- Enderle, U., Schuster, K., Prodehl, C., Schultze, A., Briebach, J., 1998. The refraction seismic experiment GRANU’95 in the Saxothuringian belt, southeastern Germany. *Geophys. J. Int.* 133, 245–259.
- Etzold, F., 1919. Die sächsischen Erdbeben während der Jahre 1907–1915. *Abhandlungen der mathematisch-physikalischen Klasse der Sächsischen Gesellschaft der Wissenschaften*, XXXVI, Nr. III. Teubner, Leipzig (B.G.).
- Faber, E., Horálek, J., Boušková, A., Teschner, M., Koch, U., Poggenburg, J., 2009. Continuous gas monitoring in the west bohemian earthquake area, Czech Republic: first results. *Stud. Geophys. Geod.* 53, 315–328.
- Fiala, J., Vejnar, Z., 2004. The lithology, geochemistry, and metamorphic gradation of the crystalline basement of the Cheb (Eger) Tertiary Basin, Saxothuringian Unit. *Bull. Geosci.* 79, 41–52.
- Fischer, T., 2003. The August–December 2000 earthquake swarm in NW Bohemia: the first results based on automatic processing of seismograms. *J. Geodyn.* 35, 59–81.
- Fischer, T., 2005. Modeling of multiple-events using empirical Greens functions: method, application to swarm earthquakes and implications for their rupture propagation. *Geophys. J. Int.* 163, 991–1005. <http://dx.doi.org/10.1111/j.1365-246X.2005.02739.x>.
- Fischer, T., Bachura, M., 2013. Detection capability of the West Bohemia seismic network based on seismic noise analysis and minimum magnitude estimate. *J. Seismol.* (accepted for publication).
- Fischer, T., Guest, A., 2011. Shear and tensile earthquakes caused by fluid injection. *Geophys. Res. Lett.* 38. <http://dx.doi.org/10.1029/2010GL045447> (L05307).
- Fischer, T., Horálek, J., 2003. Space-time distribution of earthquake swarms in the principal focal zone of the NW Bohemia/Vogtland seismoactive region. *J. Geodyn.* 35, 125–144.
- Fischer, T., Horálek, J., 2005. Slip-generated patterns of swarm microearthquakes from West Bohemia/Vogtland (central Europe): evidence of their triggering mechanism. *J. Geophys. Res.* 110, B05S21. <http://dx.doi.org/10.1029/2004JB003363>.
- Fischer, T., Michálek, J., 2008. Post 2000–swarm microearthquake activity in the principal focal zone of West Bohemia/Vogtland: space-time distribution and waveform similarity analysis. *Stud. Geophys. Geod.* 52, 493–511.
- Fischer, T., Kalenda, P., Skalský, L., 2006. Weak tidal correlation of NW-Bohemia/Vogtland earthquake swarms. *Tectonophysics* 424, 259–269.
- Fischer, T., Hainzl, S., Dahm, T., 2009. Asymmetric hydraulic fracture as a result of driving stress gradients. *Geophys. J. Int.* 179, 634–639.
- Fischer, T., Horálek, J., Michálek, J., Boušková, A., 2010. The 2008–West Bohemia earthquake swarm in the light of the WEBNET network. *J. Seismol.* 14, 665–682.
- Fischer, T., Štěpánčíková, P., Karousová, M., Tábořík, P., Flechsig, C., Gaballah, M., 2012. Imaging the Mariánské Lázně Fault (Czech Republic) by 3-D ground-penetrating radar and electric resistivity tomography. *Stud. Geophys. Geod.* 56, 1019–1036. <http://dx.doi.org/10.1007/s11200-012-0825-z>.
- Flechsig, C., Fabig, T., Rücker, C., Schütze, C., 2010. Geoelectrical investigations in the Cheb Basin/W-Bohemia: an approach to evaluate the near-surface conductivity structure. *Stud. Geophys. Geod.* 54, 443–463.
- Gautheron, C., Moreira, M., Allègre, C., 2005. He, Ne and Ar composition of the European lithospheric mantle. *Chem. Geol.* 217, 97–112.
- Gaždová, R., Novotný, O., Málek, J., Valenta, J., Brož, M., Kolínský, P., 2011. Groundwater level variations in the seismically active region of western Bohemia in the years 2005–2010. *Acta Geodyn. Geomater.* 8 (No. 1 (161)), 17–27.
- Geissler, W.H., Kämpf, H., Bankwitz, P., Bankwitz, E., 2004. The Quaternary tephra–tuff deposit of Mýtina (southern rim of the western Eger Graben/Czech Republic): indications for eruption and deformation processes (in German with summary in English). *Z. Geol. Wiss.* 32 (1), 31–54.
- Geissler, W.H., Kämpf, H., Kind, R., Klinge, K., Plenefisch, T., Horálek, J., Zedník, J., Nehybka, V., 2005. Seismic structure and location of a  $\text{CO}_2$  source in the upper mantle of the western Eger rift, Central Europe. *Tectonics* 24 (TC5001). <http://dx.doi.org/10.1029/2004TC001672>.
- Geissler, W., Kämpf, H., Seifert, W., Dulski, P., 2007. Seismic and petrological studies of the lithosphere in the earthquake swarm region Vogtland/NW-Bohemia, Central Europe. *J. Volcanol. Geoth. Res.* 159, 33–69.
- Gephart, J.W., Forsyth, D.W., 1984. An improved method for determining the regional stress tensor using earthquake focal mechanism data: application to the San Fernando earthquake sequence. *J. Geophys. Res.* 89, 9305–9320.
- Grad, M., Guterch, A., Mazur, S., Keller, G.R., Špičák, A., Hrubcová, P., Geissler, W.H., 2008. Lithospheric structure of the Bohemian Massif and adjacent Variscan belt in central Europe based on profile S01 from the SUDETES 2003 experiment. *J. Geophys. Res.* 113. <http://dx.doi.org/10.1029/2007JB005497> (B10304).
- Granet, M., Wilson, M., Achauer, U., 1995. Imaging a mantle plume beneath the French Massif Central. *Earth Planet. Sci. Lett.* 136, 281–296.
- Hainzl, S., 2004. Seismicity patterns of earthquake swarms due to fluid intrusion and stress triggering. *Geophys. J. Int.* 159, 1090–1096.
- Hainzl, S., Fischer, T., 2002. Indications for a successively triggered rupture growth underlying the 2000 earthquake swarm in Vogtland/NW-Bohemia. *J. Geophys. Res.* 107 (B12), 2338. <http://dx.doi.org/10.1029/2002JB001865>.
- Hainzl, S., Ogata, Y., 2005. Detecting fluid signals in seismicity data through statistical earthquake modeling. *J. Geophys. Res.* 110. <http://dx.doi.org/10.1029/2004JB003247> (B05S07).

- Hainzl, S., Fischer, T., Dahm, T., 2012. Seismicity-based estimation of the driving fluid pressure in the case of swarm activity in Western Bohemia. *Geophys. J. Int.* 191, 271–281. <http://dx.doi.org/10.1111/j.1365-246X.2012.05610.x>.
- Havřík, J., 2000. Stress analyses in the epicentral area of Nový Kostel (Western Bohemia). *Stud. Geophys. Geod.* 44, 522–536.
- Heidbach, O., Tingay, M.C., Barth, A., Reinecker, J., Kurfeß, D., Müller, B., 2008. The World Stress Map Database Release. <http://dx.doi.org/10.1594/GFZ.WSM.Rel2008>.
- Heinicke, J., Koch, U., 2000. Slug flow – a possible explanation for hydrogeochemical earthquake precursors at Bad Brambach, Germany. *Pure Appl. Geophys.* 157 (10), 1621–1641.
- Heinicke, J., Fischer, T., Gaupp, R., Götze, J., Koch, U., Konietzky, H., Stanek, K.P., 2009. Hydrothermal alteration as a trigger mechanism for earthquake swarms: the Vogtland/NW Bohemia region as a case study. *Geophys. J. Int.* 178, 1–13. <http://dx.doi.org/10.1111/j.1365-246X.2009.04138.x>.
- Heuer, B., Geissler, W.H., Kind, R., Kämpf, H., 2006. Seismic evidence for asthenospheric updoming beneath the western Bohemian Massif, central Europe. *Geophys. Res. Lett.* 33. <http://dx.doi.org/10.1029/2005GL025158> (L05311).
- Heuer, B., Geissler, W.H., Kind, R., the BOHEMA working group, 2011. Receiver function search for a baby plume in the mantle transition zone beneath the Bohemian Massif. *Geophys. J. Int.* 187, 577–594.
- Hiemer, S., Rößler, D., Scherbaum, F., 2011. Monitoring the West Bohemian earthquake swarm in 2008/2009 by a seismic mini-array. *J. Seismol.* 16, 169–182. <http://dx.doi.org/10.1007/s10950-011-9256-5>.
- Horálek, J., Fischer, T., 2008. Role of crustal fluids in triggering the West Bohemia/Vogtland earthquake swarms: just what we know (a review). *Stud. Geophys. Geod.* 52, 455–478.
- Horálek, J., Fischer, T., 2010. Intraplate earthquake swarms in West Bohemia/Vogtland (Central Europe). *Jökull* 60, 67–88.
- Horálek, J., Šílený, J., 2013. Source mechanisms of the 2000-earthquake swarm in the West Bohemia/Vogtland region (Central Europe). *Geophys. J. Int.* 194, 979–999. <http://dx.doi.org/10.1093/gji/ggt138>.
- Horálek, J., Boušková, A., Hampl, F., Fischer, T., 1996. Seismic regime of the West-Bohemian earthquake swarm region: preliminary results. *Stud. Geophys. Geod.* 40, 398–412.
- Horálek, J., Fischer, T., Boušková, A., Jedlička, P., 2000. The Western Bohemia/Vogtland region in the light of the WEBNET network. *Stud. Geophys. Geod.* 44, 107–125.
- Horálek, J., Šílený, J., Fischer, T., 2002. Moment tensors of the January 1997 earthquake swarm in NW Bohemia (Czech Republic): double-couple vs. non-double-couple events. *Tectonophysics* 356, 65–85.
- Hrubcová, P., Geissler, W.H., 2009. The crust–mantle transition and the Moho beneath the Vogtland/West Bohemian region in the light of different seismic methods. *Stud. Geophys. Geod.* 53, 275–294.
- Hrubcová, P., Šroda, P., Špičák, A., Guterch, A., Grad, M., Keller, G.R., Brückl, E., Thybo, H., 2005. Crustal and uppermost mantle structure of the Bohemian Massif based on CELEBRATION 2000 data. *J. Geophys. Res.* 110. <http://dx.doi.org/10.1029/2004JB003080> (B11305).
- Hrubcová, P., Vavříčuk, V., Boušková, A., Horálek, J., 2013. Moho depth determination from waveforms of microearthquakes in the West Bohemia/Vogtland swarm area. *J. Geophys. Res.* 118, 1–17. <http://dx.doi.org/10.1029/2012JB009360>.
- Ibs-von Seht, M., Plenefisch, T., Klinge, K., 2008. Earthquake swarms in continental rifts – a comparison of selected cases in America, Africa and Europe. *Tectonophysics* 452, 66–77.
- Kafka, J., 1909. *Zemětřesení* (in Czech). In: Dalekohled, Edice, Šimáček, F. (Eds.), (Praha, 47 pp.).
- Kämpf, H., Strauch, G., Vogler, P., Michler, W., 1989. Hydrologic and hydrochemic changes associated with the December 1985/January 1986 earthquake swarm activity in the Vogtland/NW Bohemia seismic area. *Z. Geol. Wiss.* 17, 685–698.
- Kämpf, H., Geissler, W.H., Bräuer, K., 2007. Combined gas–geochemical and receiver function studies of the Vogtland/NW-Bohemia intraplate mantle degassing field Central Europe. In: Ritter, J.R.R., Christiansen, U.R. (Eds.), *Mantle Plumes – A Multidisciplinary Approach*. Springer-Verlag, Berlin-Heidelberg-New York, pp. 127–158.
- Kárník, V., 1963. Earthquake swarm in the region of Kraslice in 1962. *Stud. Geophys. Geod.* 7, 288–295.
- Kárník, V., Schenková, Z., 1987. Comparison of the 1985/1986 events in Western Bohemia with earlier Vogtland swarms. In: Procházková, D. (Ed.), *Earthquake Swarm 1985/86 in Western Bohemia*. Geophys. Inst. Czechosl. Acad. Sci., Praha, pp. 324–327.
- Knett, J., 1899. Das Erzgebirgische Swarmbeben zu Hartenberg vom 1. Jänner bis Feber 1824. *Sitzungsber. Deutsch. Naturwiss. – med. Ver. Böhmen. Lotos Prag N.F.* 19, 167–191.
- Koch, U., Heinicke, J., 2011. Seismohydrological effects related to the NW Bohemia earthquake swarms of 2000 and 2008: similarities and distinctions. *J. Geodyn.* 51, 44–52.
- Koch, U., Heinicke, J., Voßberg, M., 2003. Hydrogeological effects of the latest Vogtland–NW Bohemian swarmquake period (August to December 2000). *J. Geodyn.* 35, 107–121.
- Kohl, T., Weise, S.M., Bräuer, K., Kämpf, H., Rybach, L., Strauch, G., 1998. Kombination von thermischen und CO<sub>2</sub> Signaturen zur Bewertung grossräumiger krustaler Permeabilitätsverteilung. *Mitteilungen Deutsche Geophysikalische Gesellschaft II/1998*, 78–81.
- Kolář, P., Růžek, B., 2012. Finite seismic source parameters inferred from stopping phases for selected events of west bohemia 2000 swarm. *Acta Geodyn. Geomater.* 9, 435–447.
- Korn, M., Funke, S., Wendt, S., 2008. Seismicity and seismotectonics of West Saxony, Germany – new insights from recent seismicity observed with the Saxonian seismic network. *Stud. Geophys. Geod.* 52, 479–492.
- Krentz, O., Witthauer, B., Eilers, H., Neumann, E., 1996. General map of seismicity of Saxony (in German), scale 1:400,000, Freiberg.
- Krull, P., Schmidt, D., 1990. Geological map of German Democratic Republic, Map of the fotolininations of cosmic images, Scale 1:500,000, Berlin.
- Lees, J.M., 1998. Multiplet analysis at Coso geothermal. *Bull. Seismol. Soc. Am.* 88, 1127–1143.
- Leydecker, G., 2011. *Erdbebenkatalog für Deutschland mit Randgebieten für die Jahre 800 bis 2008*. Geol. Jahrb. 59, 1–198.
- Lund, B., Slunga, R., 1999. Stress tensor inversion using detailed microearthquake information and stability constraints: application to Ölfus in southwest Iceland. *J. Geophys. Res.* 104, 14947–14964.
- Málek, J., Horálek, J., Janský, J., 2005. One-dimensional qP-wave velocity model of the upper crust for the West Bohemia/Vogtland earthquake swarm region. *Stud. Geophys. Geod.* 49, 501–524.
- Matte, P., Maluski, H., Rajlich, P., Franke, W., 1990. Terrane boundaries in the Bohemian Massif: result of large-scale Variscan shearing. *Tectonophysics* 177, 151–170. [http://dx.doi.org/10.1016/0040-1951\(90\)90279-H](http://dx.doi.org/10.1016/0040-1951(90)90279-H).
- Michálek, J., Fischer, T., 2013. Source parameters of the 2000-swarm earthquakes in West Bohemia/Vogtland determined in spectral domain. *Geophys. J. Int.* <http://dx.doi.org/10.1093/gji/ggt286>.
- Mogi, K., 1963. Some discussions on aftershocks, foreshocks and earthquake swarms – the fracture of semi-infinite body caused by an inner stress origin and its relation to the earthquake phenomena. *Bull. Earthq. Res. Inst.* 41, 615–658.
- Molchan, G., 2005. Intervent time distribution in seismicity: a theoretical approach. *Pure Appl. Geophys.* 162 (6), 1135–1150.
- Mrlina, J., Seidl, M., 2008. Relation of surface movements in West Bohemia to earthquake swarms. *Stud. Geophys. Geod.* 52, 549–566.
- Mrlina, J., Kämpf, H., Geissler, W.H., van den Bogaard, P., 2007. Proposed Quaternary maar structure at the Czech/German boundary between Mýtina and Neualbentreuth (western Eger Rift, Central Europe): geophysical, petrochemical and geochronological indications. *Z. Geol. Wiss.* 35, 213–230.
- Mrlina, J., Kämpf, H., Kroner, C., Mingram, J., Stebich, M., Brauer, A., Geissler, W.H., Kallmeyer, J., Matthes, H., Seidl, M., 2009. Discovery of the first Quaternary maar in the Bohemian Massif, Central Europe, based on combined geophysical and geological surveys. *J. Volcanol. Geotherm. Res.* 182, 97–112. <http://dx.doi.org/10.1016/j.jvolgeores.2009.01.027>.
- Nehybka, V., Skácelová, Z., 1995. Seismotectonic analysis of the seismological measurements in the Kraslice Network. *Věstník Českého geologického ústavu* 70 (2), 97–100.
- Neunhöfer, H., 1976. Ergebnisse der instrumentellen Aufzeichnung von Mikrobeben im Vogtland nach 1962. *Z. Geol. Wiss.* 4, 1617–1629.
- Neunhöfer, H., 1998. Das Bulletin der lokalen Erdbeben im Vogtland 1962–1997 (Bulletin of the Vogtland/Western Bohemia earthquakes). *Mitt. Dtsch. Geophys. Ges.* 4, 2–7.
- Neunhöfer, H., Hemmann, A., 2005. Earthquake swarms in the Vogtland/Western Bohemia region: spatial distribution and magnitude–frequency distribution as an indication of the genesis of swarms? *J. Geodyn.* 39, 361–385.
- Parotidis, M., Rothert, E., Shapiro, S.A., 2003. Pore-pressure diffusion: a possible triggering mechanism for the earthquake swarms 2000 in Vogtland/NW-Bohemia, central Europe. *Geophys. Res. Lett.* 30, 2075. <http://dx.doi.org/10.1029/2003GL018110>.
- Peterek, A., Reuther, C.D., Schunk, R., 2011. Neotectonic evolution of the Cheb Basin (Northwestern Bohemia, Czech Republic) and its implications for the late Pliocene to Recent crustal deformation in the western part of the Eger Rift. *Z. Geol. Wiss.* 39, 335–365.
- Plenefisch, T., Klinge, K., 2003. Temporal variations of focal mechanisms in the Nový Kostel focal zone (Vogtland/NW-Bohemia) – comparison of the swarms of 1994, 1997 and 2000. *J. Geodyn.* 35, 145–156.
- Plomerová, J., Achauer, U., Babuška, V., Vecsey, L., BOHEMA, W.G., 2007. Upper mantle beneath the Eger Rift (Central Europe): plume or asthenosphere upwelling? *Geophys. J. Int.* 169, 675–682. <http://dx.doi.org/10.1111/j.1365-246X.2007.03361.x>.
- Procházková, D., 1987. Earthquake pattern in Western Bohemia. In: Procházková, D. (Ed.), *Earthquake Swarm 1985/86 in Western Bohemia*. Geophys. Inst. Czechosl. Acad. Sci., Praha, pp. 324–327.
- Prodehl, C., Mueller, S., Haak, V., 1995. The European Cenozoic Rift System, in Continental rifts: evolution, structure, tectonics. In: Olsen, K.H. (Ed.), *Dev. Geotecton.* Elsevier, pp. 133–212.
- Proft, E., 1894. Kammerbühl und Eisenbühl, die Schichtvulkane des Egerer Beckens. *Jahrb. Geol. Reichsanst. Wien* 44, 25–85.
- Rabbal, W., 1994. Seismic anisotropy at the Continental Deep Drilling Site (Germany). *Tectonophysics* 232, 329–341.
- Rabbal, W., Beilecke, T., Böhlen, T., Fischer, T., Frank, A., Hasenclever, J., Borm, G., Kück, J., Bram, K., Druivenga, G., Lüschen, E., Gebrande, H., Pujol, J., Smithson, S., 2004. Superdeep vertical seismic profiling at the KTB deep drill hole (Germany): seismic close-up view of a major thrust zone down to 8.5 km depth. *J. Geophys. Res.* 109 (B09309).
- Reutel, C., 1992. Krustenfluide in Gesteinen und Lagerstätten am Westrand der Böhmisches Masse, Göttinger Arb. Geol. Paläontol. 53. Geol. Inst., Univ. Göttingen, Göttingen, Germany.
- Ritter, J.R.R., Jordan, M., Christensen, U.R., Achauer, U., 2001. A mantle plume below the Eifel volcanic fields, Germany. *Earth Planet. Sci. Lett.* 186, 7–14.
- Růžek, B., Horálek, J., 2013. Three-dimensional seismic velocity model of the West Bohemia/Vogtland seismoactive region. *Geophys. J. Int.* 195, 1251–1266.
- Šafanda, J., Čermák, V., 2000. Subsurface temperature changes due to the crustal magmatic activity – numerical simulation. *Stud. Geophys. Geod.* 44, 327–335.
- Schenk, V., Schenková, Z., Jechumtálová, Z., 2009. Geodynamic pattern of the West Bohemia region based on permanent GPS measurements. *Stud. Geophys. Geod.* 53, 329–341.
- Seifert, W., Kämpf, H., 1994. Ba-enrichment in phlogopite of a nephelinite from Bohemia. *Eur. J. Mineral.* 6, 497–502.
- Shapiro, S.A., Huenges, E., Borm, G., 1997. Estimating the crust permeability from fluid-injection-induced seismic emission at the KTB site. *Geophys. J. Int.* 131, F15–F18.

- Šibrava, V., Havlíček, P., 1980. Radiometric age of Plio-Pleistocene volcanic rocks of the Bohemian Massif. *Věstník Ústředního Ústavu Geologického* 55, 129–139.
- Škvor, V., Sattran, V., 1974. Krušné Hory, západní část, 1:50.000, Ústřední Ústav Geologický, Praha.
- Slancová, A., Horálek, J., 2000. Analysis of the state of stress during the 1997 earthquake swarm in Western Bohemia. *Stud. Geophys. Geod.* 44, 272–291.
- Špičák, A., 1987. Fault plane solutions of 1985 Dec. 21 and 1986 Jan. 20 events. In: Procházková, D. (Ed.), *Earthquake Swarm 1985/86 in Western Bohemia*. Geophys. Inst. Czechosl. Acad. Sci, Praha, pp. 268–273.
- Špičák, A., Horálek, J., 2000. Migration of events during the January 1997 earthquake swarm (The West Bohemia–Vogtland region). *Stud. Geophys. Geod.* 44, 227–232.
- Špičáková, L., Uličný, D., Koudelková, G., 2000. Tectonosedimentary evolution of the Cheb Basin (NW Bohemia, Czech Republic) between the Late Oligocene and Pliocene: a preliminary note. *Stud. Geophys. Geod.* 44, 556–580.
- Stejskal, V., Málek, J., Novotný, O., 2008. Variations in discharge and temperature of mineral springs at the Františkovy Lázně spa, Czech Republic, during a nearby earthquake swarm in 1985/1986. *Stud. Geophys. Geod.* 52, 589–606.
- Tittel, B., Wendt, S., 2003. Magnitudes and time distribution of the swarm earthquakes August–November 2000 in NW Bohemia. *J. Geodyn.* 35, 97–105.
- Tomek, Č., Dvořáková, V., Vrána, S., 1997. Geological interpretation of the 9HR and 503M seismic profiles in Western Bohemia. In: Vrána, S., Štědrá, V. (Eds.), *Geological Model of Western Bohemia Related to the KTB Borehole in Germany*. J. Geol. Sci. Geol., 47, pp. 43–50.
- Touati, S., Naylor, M., Main, I.G., Christie, M., 2011. Masking of earthquake triggering behavior by a high background rate and implications for epidemic-type aftershock sequence inversions. *J. Geophys. Res.* 116. <http://dx.doi.org/10.1029/2010JB007544> (B03304).
- Treixler, G., 1929. *Heimatkunde des Bezirkes Graslitz [I. Band]/Herausgegeben vom Bezirks-Bildungsausschuss Graslitz, Druck von Gustav Rühle, Graslitz (269 pp.)*.
- Ulrych, J., Lloyd, F.E., Balogh, K., 2003. Age relations and geochemical constraints of Cenozoic alkaline volcanic series in W Bohemia: a review. *Geolines* 15, 168–180.
- Ulrych, J., Dostal, J., Adamovič, J., Jelinek, E., Špaček, P., Hegner, E., Balogh, K., 2011. Recurrent Cenozoic volcanic activity in the Bohemian Massif (Czech Republic). *Lithos* 123, 133–144.
- Vavryčuk, V., 1993. Crustal anisotropy from local observations of shear-wave splitting in West Bohemia, Czech Republic. *Bull. Seismol. Soc. Am.* 83, 1420–1441.
- Vavryčuk, V., 2002. Non-double-couple earthquakes of January 1997 in West Bohemia, Czech Republic: evidence of tensile faulting. *Geophys. J. Int.* 149, 364–373. <http://dx.doi.org/10.1046/j.1365-246X.2002.01654.x>.
- Vavryčuk, V., 2011a. Principal earthquakes: theory and observations from the 2008 West Bohemia swarm. *Earth Planet. Sci. Lett.* 305, 290–296. <http://dx.doi.org/10.1016/j.epsl.2011.03.002>.
- Vavryčuk, V., 2011b. Tensile earthquakes: theory, modeling, and inversion. *J. Geophys. Res.* 116. <http://dx.doi.org/10.1029/2011JB008770> (B12320).
- Vavryčuk, V., 2011c. Detection of high-frequency tensile vibrations of a fault during shear rupturing: observations from the 2008 West Bohemia swarm. *Geophys. J. Int.* 186, 1404–1414. <http://dx.doi.org/10.1111/j.1365-246X.2011.05122.x>.
- Vavryčuk, V., 2001. Inversion for parameters of tensile earthquakes. *J. Geophys. Res.* 106, 16339–16355. <http://dx.doi.org/10.1029/2001JB000372>.
- Vavryčuk, V., Boušková, A., 2008. S-wave splitting from records of local micro-earthquakes in West Bohemia/Vogtland: an indicator of complex crustal anisotropy. *Stud. Geophys. Geod.* 52, 631–650. <http://dx.doi.org/10.1007/s11200-008-0041-z>.
- Vavryčuk, V., Bouchaala, F., Fischer, T., 2013. High-resolution fault image from accurate locations and focal mechanisms of 2008 swarm earthquakes in West Bohemia, Czech Republic. *Tectonophysics* 590, 189–195. <http://dx.doi.org/10.1016/j.tecto.2013.01.025>.
- Vylita, T., Žák, K., Čílek, V., Hercman, H., Mikšíková, L., 2007. Evolution of hot-spring travertine accumulation in Karlovy Vary/Carlsbad (Czech Republic) and its significance for the evolution of Tepla valley and Ohře/Eger rift. *Z. Geomorphol. N.F.* 51, 427–442.
- Wagner, G.A., Gögen, K., Jonckheere, R., Wagner, I., Woda, C., 2002. Dating of Quaternary volcanoes Komorní hůrka (Kammerbühl) and Železná hůrka (Eisenbühl), Czech Republic, by TL, ESR, alpha-recoil and fission track chronometry. *Z. Geol. Wiss.* 30, 191–200.
- Weinlich, F.H., Bräuer, K., Kämpf, H., Strauch, G., Tesar, J., Weise, S.M., 1999. An active subcontinental mantle volatile system in the western Eger rift, Central Europe: gas flux, isotopic (He, C, and N) and compositional fingerprints. *Geochim. Cosmochim. Acta* 63, 3653–3671. [http://dx.doi.org/10.1016/S0016-7037\(99\)00187-8](http://dx.doi.org/10.1016/S0016-7037(99)00187-8).
- Wendt, J., Dietrich, R., 2003. Determination of recent crustal deformations based on precise GPS measurements in the Vogtland earthquake area. *J. Geodyn.* 35, 235–246.
- Wilde-Piorko, M., Saul, J., Grad, M., 2005. Differences in the crustal and uppermost mantle structure of the Bohemian Massif from teleseismic receiver functions. *Stud. Geophys. Geod.* 49, 85–107.
- Wyss, M., Shimazaki, K., Wiemer, S., 1997. Mapping active magma chambers by b values beneath the off-Ito volcano, Japan. *J. Geophys. Res.* 102 (B9), 20,413–20,422.
- Zahradník, J., Plešinger, A., 2010. Toward understanding subtle instrumentation effects associated with weak seismic events in the near field. *Bull. Seismol. Soc. Am.* 100, 59–73.
- Zahradník, J., Anonini, M., Grünthal, G., Janský, J., Procházková, D., Schmedes, E., Špičák, A., Zedník, J., 1990. A combined study of macroseismic data and focal mechanisms applied to the West-Bohemian Earthquake, Czechoslovakia. *Pure Appl. Geophys.* 133, 53–71.